NRL Report 7460

A Review of the Plane-Stress Fracture Mechanics Parameter K_c Determined Using the Center-Cracked Tension Specimen

A. M. SULLIVAN AND C. N. FREED

Strength of Metals Branch
Metallurgy Division

December 29, 1972

NAVAL RESEARCH LABORATORY
Washington, D.C.

Approved for public release; distribution unlimited.

PREFACE

This review of thin-sheet testing using the center-cracked tensile (CCT) specimen was prepared as part of a general review of thin-sheet testing for the Thin Sheet Task Group of ASTM Committee E-24:01. The general review is to provide guidance for the committee in formulating a standard for thin-sheet testing and incorporates other pertinent topics by authors from other laboratories. However, since this review (as well as the others) will be edited and condensed by the Task Group Chairman for presentation to the Committee, it seems appropriate to publish this unabridged version for reference purposes.

Although quite comprehensive, this review does not purport to be all-inclusive, since the illustrations are drawn largely from NRL research and reports.

CONTENTS

Abstract iii
Problem Status iii
Authorization iii

INTRODUCTION 1

CHARACTERISTICS OF THE PLANE-STRESS FRACTURE RESISTANCE K_c 2

Geometrical Dependencies of K_c 2
Temperature and Rate Dependency 6

EXPERIMENTAL PARAMETERS 6

Test Specimen 6
Notch Preparation 7
Loading Arrangements 7
Buckling Restraint 7
Load Measurement 7
Crack-Length Measurement 7

EXPERIMENTAL PARAMETERS AT NRL 11

Test-Specimen Dimensions 11
Notch Preparation 11
Loading Arrangements 12
Buckling Restraints 12
Load Measurement 12
Crack-Length Measurement 13
Calibration Procedure 13
Data Reduction 18

EXPERIMENTAL PARAMETERS AT OTHER LABORATORIES 19

DATA ANALYSIS AT NRL 20

Effect of Specimen Width on K_c 20
Effect of Crack-Length-to-Width Ratio 20
Effect of Sheet Thickness 20
Effect of Notch Root Radius on K_c 29
Definition of Instability 30

CONCLUSIONS 31

RECOMMENDATIONS 31

REFERENCES 32

APPENDIX — Questionnaire and Answers 35

A REVIEW OF THE PLANE-STRESS FRACTURE MECHANICS PARAMETER K_c DETERMINED USING THE CENTER-CRACKED TENSION SPECIMEN

INTRODUCTION

After the ASTM-sponsored symposium on "Fracture Toughness Testing and Its Applications" in 1964, [later published as ASTM STP 381 (1)], a resurgence of interest in thin-sheet testing seemed to occur. In part, of course, this development came about from the fact that a tentative method for plane-strain testing had been formulated, but it was also realized that the experience gained in K_{Ic} testing could serve to eliminate some of the pitfalls experienced in earlier plane-stress-K_c experimentation.

Alcoa, under Kaufman, began thin-sheet testing in 1964 (2) and has continued to date, incorporating K_c values for aluminum alloys in its Aerospace Technical Bulletin Series.

At about the same time, Broek in Holland at the National Aerospace Laboratory started to produce a series of reports on center-cracked-tensile (CCT) thin-sheet testing, discussed as residual strength, which continues to date (3-8).

Frankford Arsenal delivered a paper at the First International Conference on Fracture in 1965 (9) showing a continuing interest in thin-sheet work. A long tradition of collaboration between Frankford Arsenal and NRL has resulted in much fruitful work, in part stimulated by Irwin's interest in K_c testing. This has continued to date with several coauthored papers resulting (10,11).

Although not published until 1966, a report discussing specimen dimensions and buckling effects from the AF Flight Dynamics Laboratory at Wright Patterson Air Force Base (12) summarizes work done in 1960-61.

Later, at the ASTM-sponsored symposium on "Damage Tolerance in Aircraft," 1970, [published as ASTM STP 486 (13)], considerable thin-sheet data were included (14,15) together with one paper discussing the use of K_c data in aircraft design (16).

The Naval Research Laboratory (Metallurgy Division) began an experimental program on CCT thin-sheet testing in 1970, which has so far published K_c data on aluminum-, titanium-, and steel-alloy sheet material (17-24).

The fact that so much material has appeared over the last decade indicates a significant current interest in thin-sheet testing; in turn this presages that, as these efforts are correlated and channeled, specifications can be developed to ensure the production of valid K_c data to be incorporated in fail-safe design practices.

CHARACTERISTICS OF THE PLANE-STRESS FRACTURE RESISTANCE K_c

Geometrical Dependencies of K_c

The geometrical dependencies of fracture resistance are not unique to the CCT specimen. Sufficient constraint must be provided to maintain essentially elastic conditions at the crack tip. This means that varying the ratio K_c/σ_{ys} requires variation in the sheet width to produce valid data. The crack-length-to-width ratio 2a/W is also an important variable, valid data being produced only over a specific range of this ratio. These restrictions are combined with the obvious one: that in no instance must the net section stress exceed the yield stress of the material. The three-dimensional diagram of Fig. 1 illustrates the effect of the above-mentioned variables, width and the crack-length-to-width ratio.

Sheet thickness is also an important variable. Examination of profiles of fractures over a thickness series has indicated that when the profile was entirely square, K_c has reached a minimum value and is no longer thickness dependent. With reduced thickness, lesser amounts of flat fracture and a proportionally greater degree of shear lip was observed (at higher K_c values) until an entirely "slant" fracture was developed. These shapes are sketched in Figs. 2 and 3.

The Roman numeral I was assigned to the square fracture, signifying opening mode fracture and considered to be a predominantly plane-strain situation. Two other modes, II and III, were described (25,26) as "shear normal to the leading edge of the crack" (plane strain or plane stress) and "shear parallel to the leading edge of the crack" (anti-plane strain). These are illustrated in Figs. 4 and 5. It must now be recognized that in specimens too thin to develop plane-strain fracture only, the proportion of plane strain to plane stress will vary with thickness; this is indicative of indeterminate relative amounts

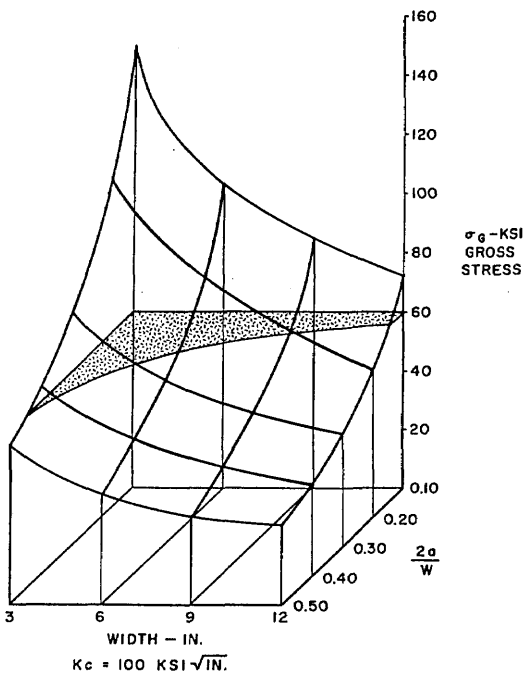

Fig. 1 — Three-dimensional representation of specimen width W and crack-length-to-width ratio 2a/W for a hypothetical alloy having a K_c value of 100 ksi $\sqrt{\text{in.}}$, the sloping surface area. The hatched plane parallel to the base separates the upper region, where yielding has occurred, from the lower, where yielding has not occurred and from which valid K_c data may be obtained. (Ref. 19; Fig. 2)

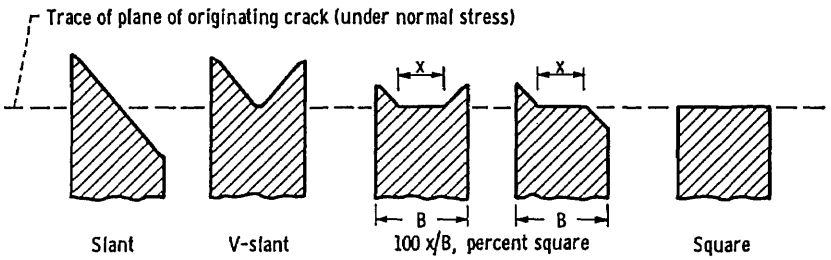

Fig. 2a — Recommended descriptive terms for types of fracture surfaces observed in plate specimens illustrated in section views taken normal to the direction of propagation. [From ASTM Special Technical Publication No. 381, Fig. 5, Page 142, published by the Am. Soc. for Testing and Materials, 1965. Used by permission.]

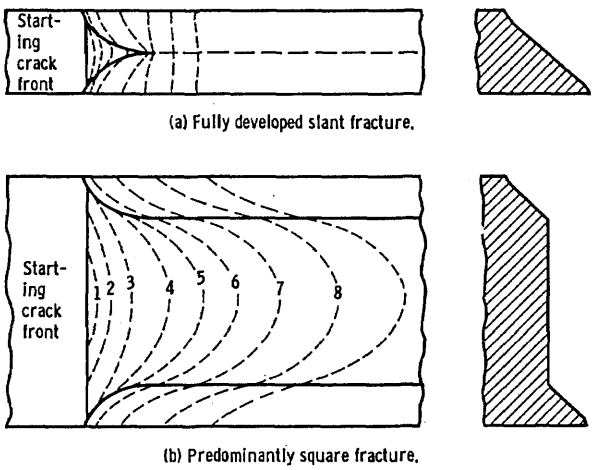

Fig. 2b — Schematic drawing of various successive positions of crack fronts shown as dashed lines in specimens having (A) fully developed slant fracture or (B) predominantly square fracture (about 70 percent square.) [From ASTM Special Technical Publication No. 381, Fig. 6, Page 143, published by the Am. Soc. for Testing and Materials, 1965. Used by permission.]

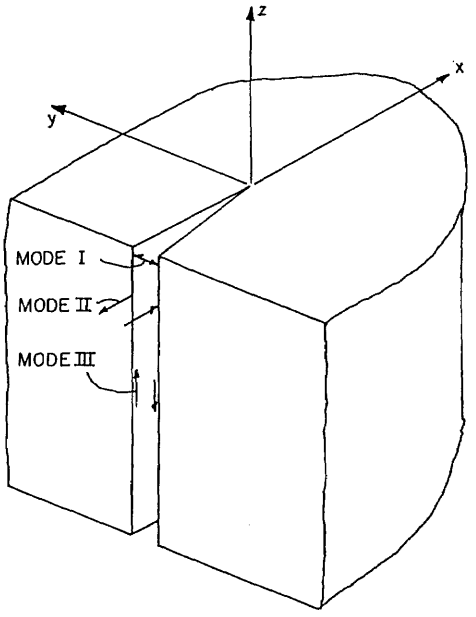

Fig. 3a — Modes of deformation of a crack. [From ASTM Special Technical Publication No. 381, Fig. 2, Page 86, published by the Am. Soc. for Testing and Materials, 1965. Used by permission.]

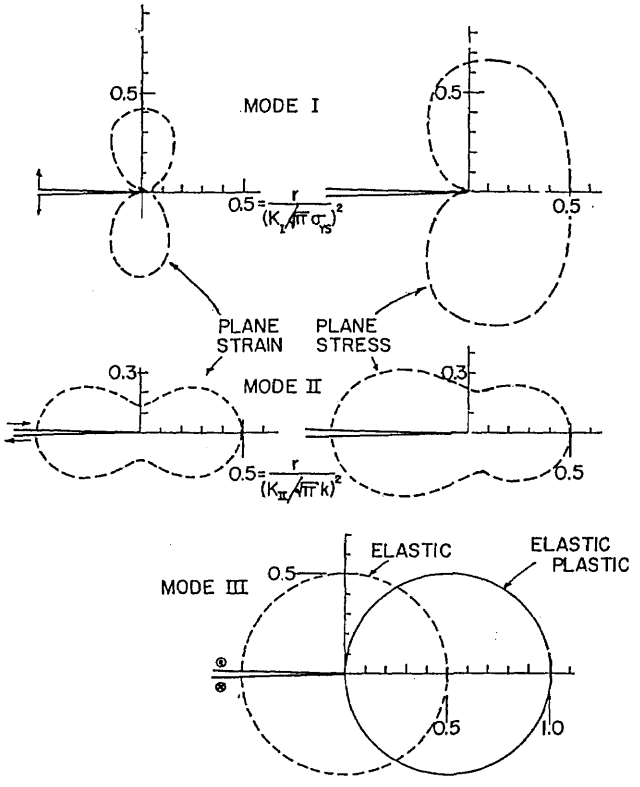

Fig. 3b — Elastic stress singularities of the different crack deformation modes viewed in terms of Mises' yield-limit lines. Poisson's ratio is assumed to be 1/3. [From ASTM Special Technical Publication No. 381, Fig. 3, Page 87, published by the Am. Soc. for Testing and Materials, 1965. Used by permission.]

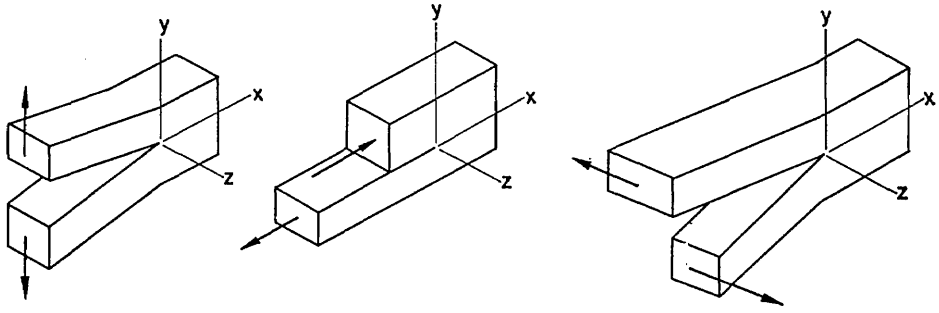

Fig. 4a — The basic modes of crack surface displacements. [From ASTM Special Technical Publication No. 381, Fig. 1, Page 31, published by the Am. Soc. for Testing and Materials, 1965. Used by permission.]

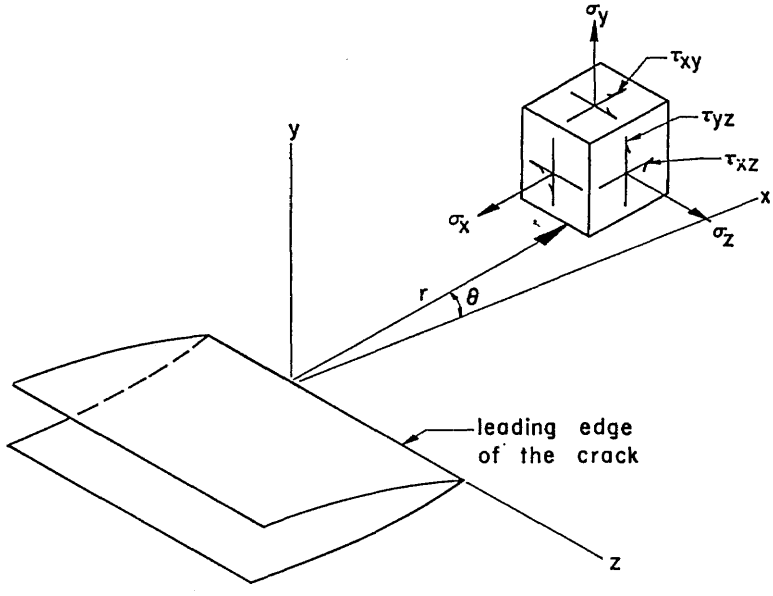

Fig. 4b — Coordinates measured from the leading edge of a crack and the stress components of the crack-tip stress field. [From ASTM Special Technical Publication No. 381, Fig. 2, Page 31, published by the Am. Soc. for Testing and Materials, 1965. Used by permission.]

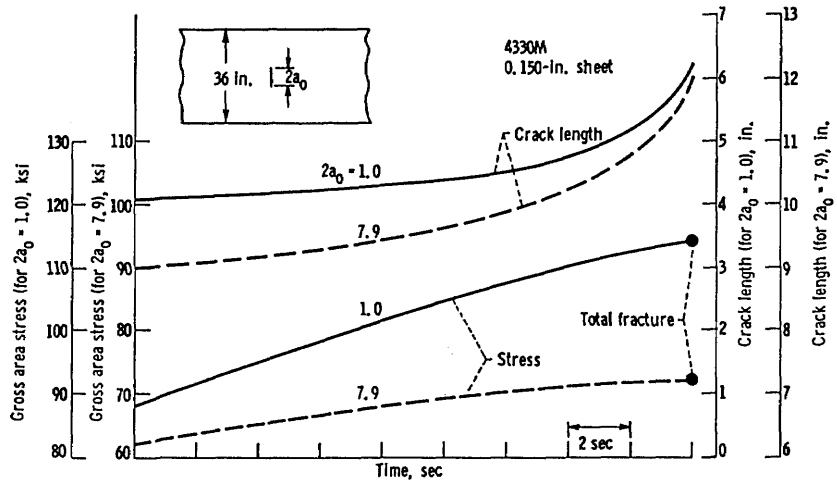

Fig. 5 — Examples of stress and crack-length measurements using cinematography. [From ASTM Special Technical Publication No. 381, Fig. 21, Page 174, published by the Am. Soc. for Testing and Materials, 1965. Used by permission.]

of modes II and III shear. Thus K_{Ic} can be evaluated independent of specimen thickness, but K_c can neither be precisely defined nor separated from thickness effects.

This survey of dimensional dependency leads to several inescapable conclusions: (a) for valid linear elastic fracture mechanics (LEFM) testing, no standard-sized specimen can be designed which will produce valid data over the full range of toughness, width, and thickness variation; (b) in the K_c thickness range, testing must be performed on material of the specific thickness required for structural application.

Temperature and Rate Dependency

Because of the observed geometric effect and subsequent early emphasis on plane-strain toughness measurement, plane-stress temperature or rate dependencies have been largely neglected. However, known variations in material properties not only affect fracture toughness but, through constraint alterations, also change the specimen-size requirement. Therefore, serious research must include these parameters in any test program. Efforts in this direction have been begun by Broek (5).

EXPERIMENTAL PARAMETERS

Specimen-preparation guidelines and experimental procedures are considered in the following.

Test Specimen

The requirement for variously sized CCT specimens has been that the length L should be three times the width W.

Notch Preparation

Critical features of notch preparation include exact symmetry of location, width (recommended as 0.0625 in.), and notch-tip root radius. Various methods can be used for notch insertion: jeweler's saw cut, machining, or an electric-discharge method.

These methods all produce an artificial notch tip, whereas the sharper so-called natural crack is the starting point for service failure. Ideally, therefore, the notch tip should be extended by fatigue in tension — tension loading at reasonably low load levels (27) to minimize the size of the thus produced plastic zone. However, it is true that where some crack growth can be expected, the effects of the artificial notch tip are largely minimized (7,28).

Loading Arrangements

The specimens must be pin loaded; therefore some gripping arrangement must be attached to the specimen ends sufficiently sturdy to accommodate a yoke-and-pin loading device on the testing machine. Also, since length, which is proportional to width, must be considered, such attachments (particularly for the wider specimens) commonly require testing machines of unusually high head capacity.

Buckling Restraint

A thin sheet has a tendency to buckle as the crack grows; the relative-thickness dimension B at which this will occur depends somewhat on fracture resistance, specimen size, and initial crack length. Since this buckling seriously affects the validity of the K_c value, face plates should be affixed to the central section of the specimen and fitted close to the crack path. Lubrication should be provided for the inner surfaces; some inert type, such as Teflon, known not to produce stress corrosion effects, is suitable.

Load Measurement

Since the determination of K_c requires knowledge of the stress and crack length at failure, any method which provides a load measurement directly correlated to the crack length is satisfactory.

Crack-Length Measurement

The original slit length $2a_0$, which may be relevant to crack-growth resistance, can be measured after fracture, since the fatigue crack tip is readily measured. Where no fatigue crack is present, the machined surface similarly provides a reference.

Measurement of the final crack length a_c at instability is difficult. Despite the fact that there are differences in fracture appearance between "slow growth" and "fast fracture," these are both ill defined and material dependent, so that in practice no demarcation is adequately identifiable. Direct measurement of the growing crack must be made, and this must be in tandem with instantaneous load measurement.

A brief review of six procedures follows in detail. Since this is condensed from the Srawley-Brown monograph (29), only certain necessary individual references are cited.

Ink Staining — This early "historical method" is highly unsatisfactory. First efforts involved a sequence of colored inks. As the crack grew, the specimen was periodically unloaded, inked, and allowed to dry. After reloading the specimen at intervals, the above procedure was repeated (30). The increasing velocity of "slow" growth toward the region of instability, however, ensures this to be a peculiarly unsatisfactory method for precise crack-length determination.

An outgrowth of this was the recommendation (31) that a small quantity of ink be pipetted into the notch tip. During slow growth, capillarity ensures coverage of the fracturing surface; at instability, staining can no longer follow the fast-moving crack so that the length of the inked surface may be measured. However, this method is also imprecise, due to spattering effects. Further, the action of the staining medium in providing a potential stress-corrosion situation is hardly debatable.

Photography — Paired motion-picture cameras can be synchronized to simultaneously photograph the testing-machine load dial and the fracturing region of the plate. Refinements of this technique include polarizing screens to minimize reflections, lighting adjustments, and different optical systems (32). Crack length is then measured directly by frame-to-frame examination of the film. Crack length at instability is determined either by plotting it against stress or together with stress against frame number or time. Typical data are provided in Fig. 5. This technique has been successfully employed by the aircraft industry, particularly for very wide thin sheets.

Disadvantages include the tedious single-frame measurements and the fact that since total fracture may occur between two frames, the absolute value of 2a may be in error. Use of high-speed cameras precludes the latter but in turn may not include the slow-crack-growth portion; triggering can also be a problem.

Electric Potential — Since disturbance of a potential field in the region of a discontinuity exists in a current-carrying body, when constant current is supplied, the potential difference between two fixed points spanning a crack will increase as the crack extends. Calibration curves similar to those for the displacement gage can be used for crack-length determination (Fig. 6). Plots of load vs potential can be obtained by feeding the output of a voltmeter amplifier to one channel of an XY recorder and by feeding the load-cell signal to the other channel; typical curves are provided in Fig. 7. The technique is readily adapted to all specimen types, and very high sensitivity to crack extension may be obtained (0.0025 in.).

Acoustic Emission — A transducer converting an elastic vibration into an electric signal can be used to monitor within a material a disturbance such as a sudden release of elastic energy (33). Thus signals from a piezoelectric crystal in contact with a specimen containing a propagating crack may be amplified and recorded.

The simplicity and adaptability of this system make it an attractive one; however, there is considerable ambiguity in the interpretation of the output signals. In conjunction with another crack measuring system, acoustic signals may serve as an aid to their interpretation (Fig. 8), but as yet there is no sure way of estimating the amount of crack extension from acoustic records.

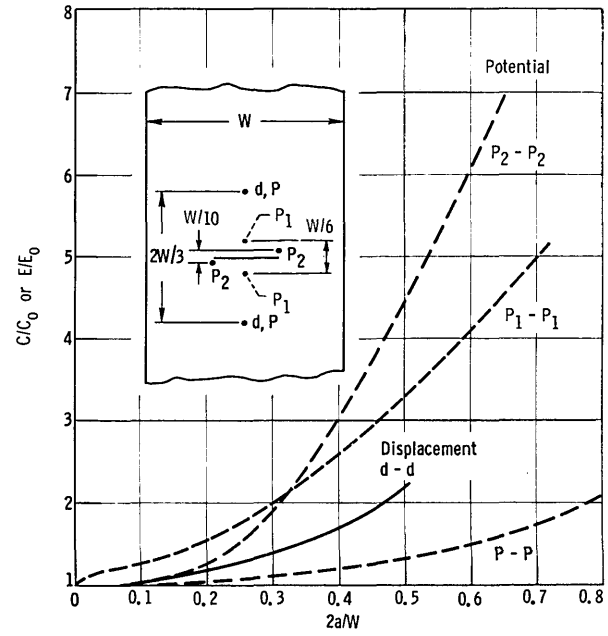

Fig. 6a — Comparison of the displacement-gage calibration curve with several calibration curves obtained by using electric-potential measurements illustrating the influence of gage length. [From ASTM Special Technical Publication No. 381, Fig. 27, Page 183, published by the Am. Soc. for Testing and Materials, 1965. Used by permission.]

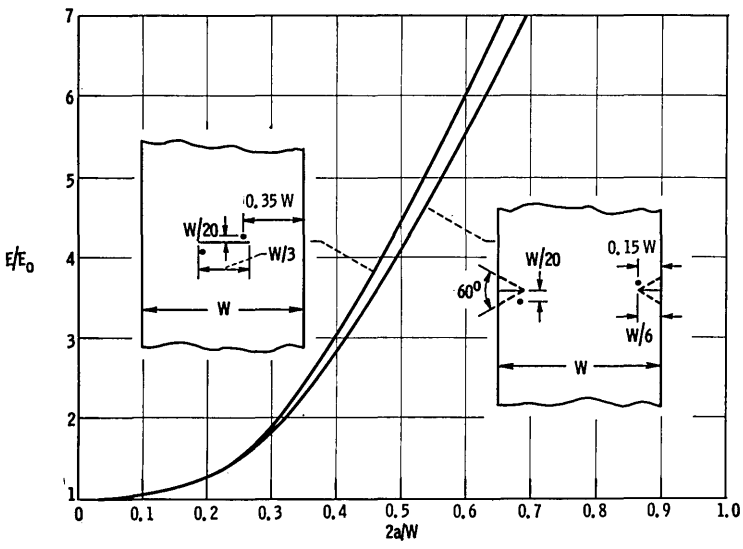

Fig. 6b — Electric-potential calibration curves for symmetrically center- and edge-cracked plate specimens. [From ASTM Special Technical Publication No. 381, Fig. 23, Page 177, published by the Am. Soc. for Testing and Materials, 1965. Used by permission.]

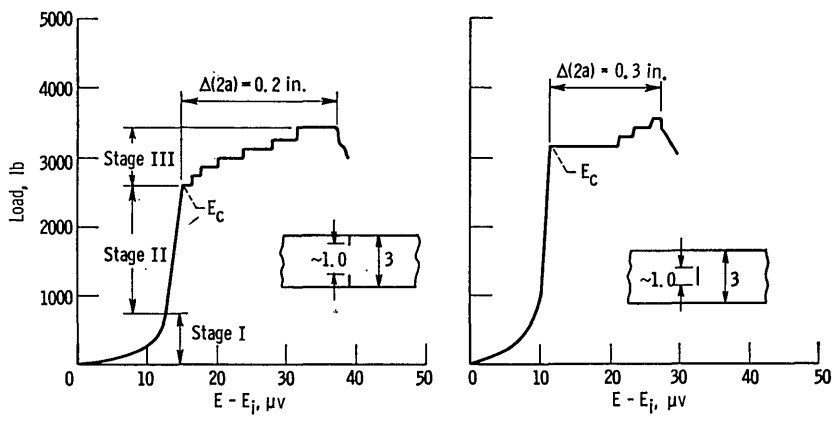

Fig. 7 — Typical load vs potential records illustrating pop-in and crack extension to maximum load. [From ASTM Special Technical Publication No. 381, Fig. 22, Page 176, published by the Am. Soc. for Testing and Materials, 1965. Used by permission.]

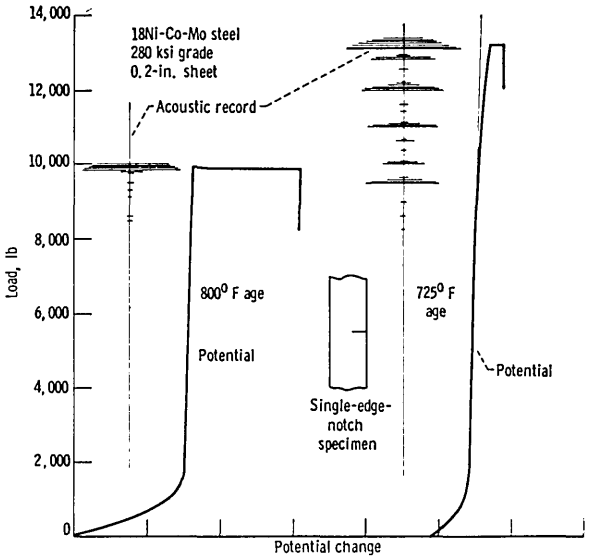

Fig. 8 — Load-potential and acoustic records from single-edge notched specimens illustrating different pop-in behavior. [From ASTM Special Technical Publication No. 381, Fig. 28, Page 186, published by the Am. Soc. for Testing and Materials, 1965. Used by permission.]

Continuity Gage — This special type of strain gage consists of regularly spaced ribbon elements connected in parallel. It provides essentially linear resistance change as successive elements are fractured by the growing crack.

Displacement Gage — The relationship of K to changes in the spring constant with crack length suggested the development of a compliance gage (34). Displacement is measured directly, and crack length can be evaluated from a calibration curve relating the crack length to the spring constant. Dimensions of the test specimen must, of course, be proportioned to those of the calibration specimen.

Simpler variations of this form of gage can be beam or clip gages provided with a wire resistance or foil gages on opposite faces. When such gages are bent to bear against two reference surfaces across the crack, the crack opening will give values of crack length 2a when referred to appropriate calibrations (35). For these applications, gage linearity and sensitivity are paramount considerations; appropriate recording circuitry must also be available.

An Intercomparison — The dependency of K values on both temperature and strain rate requires measurement procedures applicable under the restricted conditions of such tests. Excluding ink staining, a method of purely historical interest in crack-length measurement, degrees of suitability of the other test methods have been implied in the appropriate discussions. These, however, related simply to static testing under ambient-temperature conditions; their application to other test conditions is considered here.

Photography is obviously unsuitable for tests at other than ambient temperatures, since the temperature-sustaining apparatus would interfere with visual observation of the advancing crack.

Electric-potential measurement is adequate only over a limited temperature range. Resistance decreases rapidly with lowered temperature, thus requiring a prohibitively large current even for the smaller specimens designed to measure K_{Ic}; at elevated temperatures, thermoelectric effects become appreciable. Further, the testing speed is limited by the response of the potential-measuring device. A high-sensitivity electric voltmeter gives a response speed of only 0.5 s, and the use of an oscilloscope is apparently not possible because suitable input are not available amplifiers.

Acoustic-emission measurement is quite practical for both low-temperature and high-speed testing but expensive at best and not adaptable to crack extensions greater than 0.2 in.

Thus, for versatility, displacement-gage techniques can be considered the most suitable, since these could be employed under any combination of testing conditions: varied temperature and varied rate.

EXPERIMENTAL PARAMETERS AT NRL

The broad program of thin-sheet testing inaugurated at NRL in 1969 had two definitive objectives:

- To assist in the development of a standard testing procedure for the determination of K_c, the plane-stress fracture mechanics parameter for a thin sheet.

- To provide fracture-resistance data for a broad spectrum of high-strength sheet alloys of aluminum, titanium, and steel over a wide range of gage thickness.

Consequently, some procedures were adopted specifically to further the second objective.

Test-Specimen Dimensions

At present the "standard" test specimen has a width of 12 in. Such a specimen is shown in the tensile machine in Fig. 9. Other widths (3, 6, 9, 10, 15, and 20 in.) have been used for verifying the results using the 12-in. width. Choice of specimen width depends on an estimate of K_c/σ_{ys}.

Notch Preparation

An electric-discharge method, Elox, has been employed almost exclusively. It proved most practical because not only were the notches inserted most rapidly, but it was the least expensive method.

No facilities are presently available at NRL for fatiguing the CCT specimens. A shim stock electrode is used to produce a narrow-crack-tip extension by Elox; these are 0.002 in. wide, with tip radii of 0.001 in.

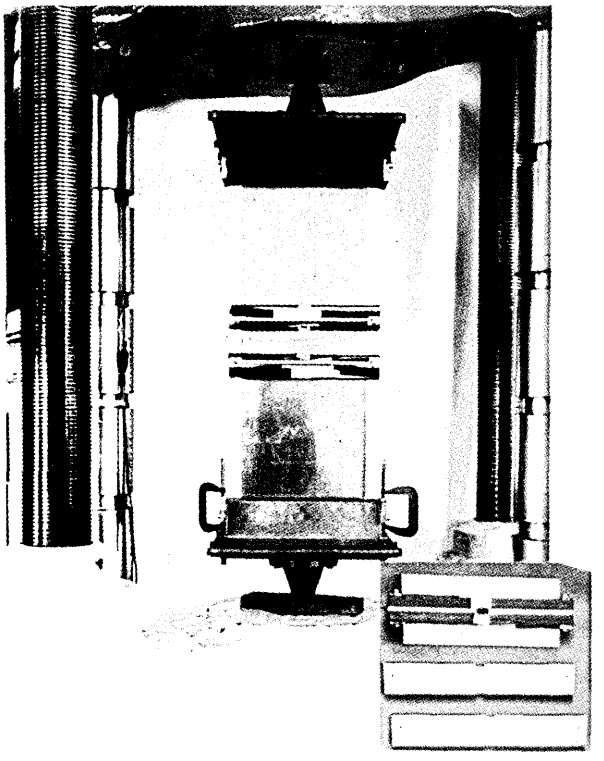

Fig. 9 — A typical center-crack tensile specimen (CCT-NRL) in the testing machine (Ref. 17; Fig. A1)

Loading Arrangements

The specimen was bolted to a head piece which was pin loaded through a device arrangement.

Buckling Restraint

When panels containing slits longer than 2 in. were loaded, the specimen manifested a tendency to buckle. This is inadmissible, since it perturbs the stress field at the slit tips in a manner not predicted by the analytic expression employed for computation. Therefore, to suppress buckling, split aluminum face plates, 12 in. long by 2 in. wide by 0.5 in. thick, were employed. The faces of the plates were covered with Teflon, and the backs were made rigid with an aluminum T-shaped section.

Load Measurement

Since the load and crack length were to be monitored simultaneously, some method of transferring load measurement to an XY recorder was desirable. Accordingly, a microformer attachment was fitted to the load train of the testing machine (Baldwin, capacity 400,000 lb), and its output was fed to the Y channel of a Moseley (Hewlett Packard) recorder.

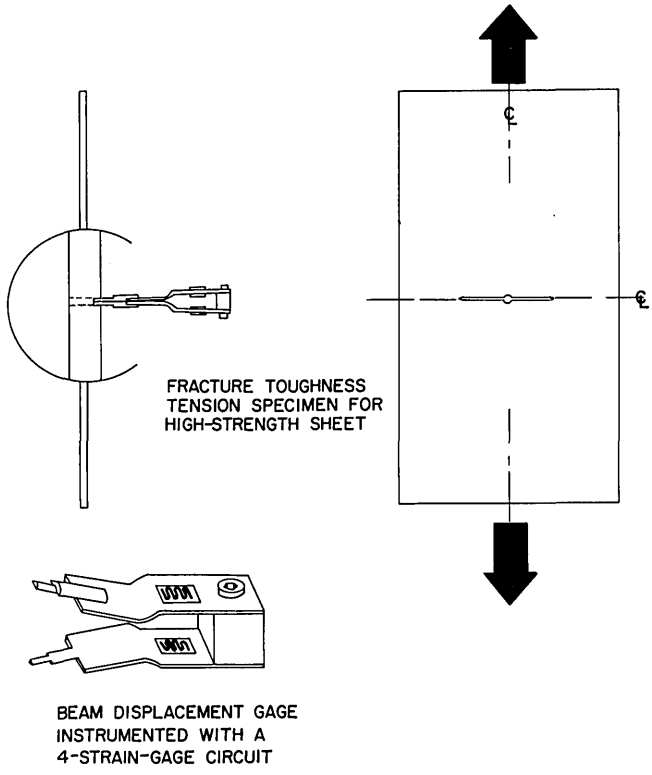

Fig. 10 — Center-crack tensile specimen (CCT-NRL) with drawing of probe used for the crack-opening measurement. (Ref. 17; Fig. 1)

Crack-Length Measurement

Instantaneous crack length is measured directly by a displacement-gage probe. This probe, depicted in Fig. 10, measures the crack-opening displacement (COD) of a 0.1875-in.-diameter hole in the center of the Eloxed slit. The output from the 4-gage bridge circuit is displayed on the X channel of the Moseley recorder. These COD measurements are then converted to crack lengths by reference to a normalized $E[COD]/\sigma_W$-vs-2a/W calibration curve.

Calibration Procedure

To monitor the growing crack by COD measurements, a calibration against crack length was made. Specimens of 7178-T6 aluminum were prepared with the following dimensions: length 36 in.; width 12 in.; thickness 0.063 in. Initial slits, 0.063 in. wide, were prepared by an electric-discharge method; slit lengths used for calibration were 1.2, 2, 3, 4, 5, 6, and 7 in.

The COD measurement was done with the aforementioned strain-gage-instrumented probe having semicircular tips, (Fig. 11) which fit into a 0.188-in. hole drilled at the slit center. This permitted positioning the face plates quite close to the slit lip. Signals from

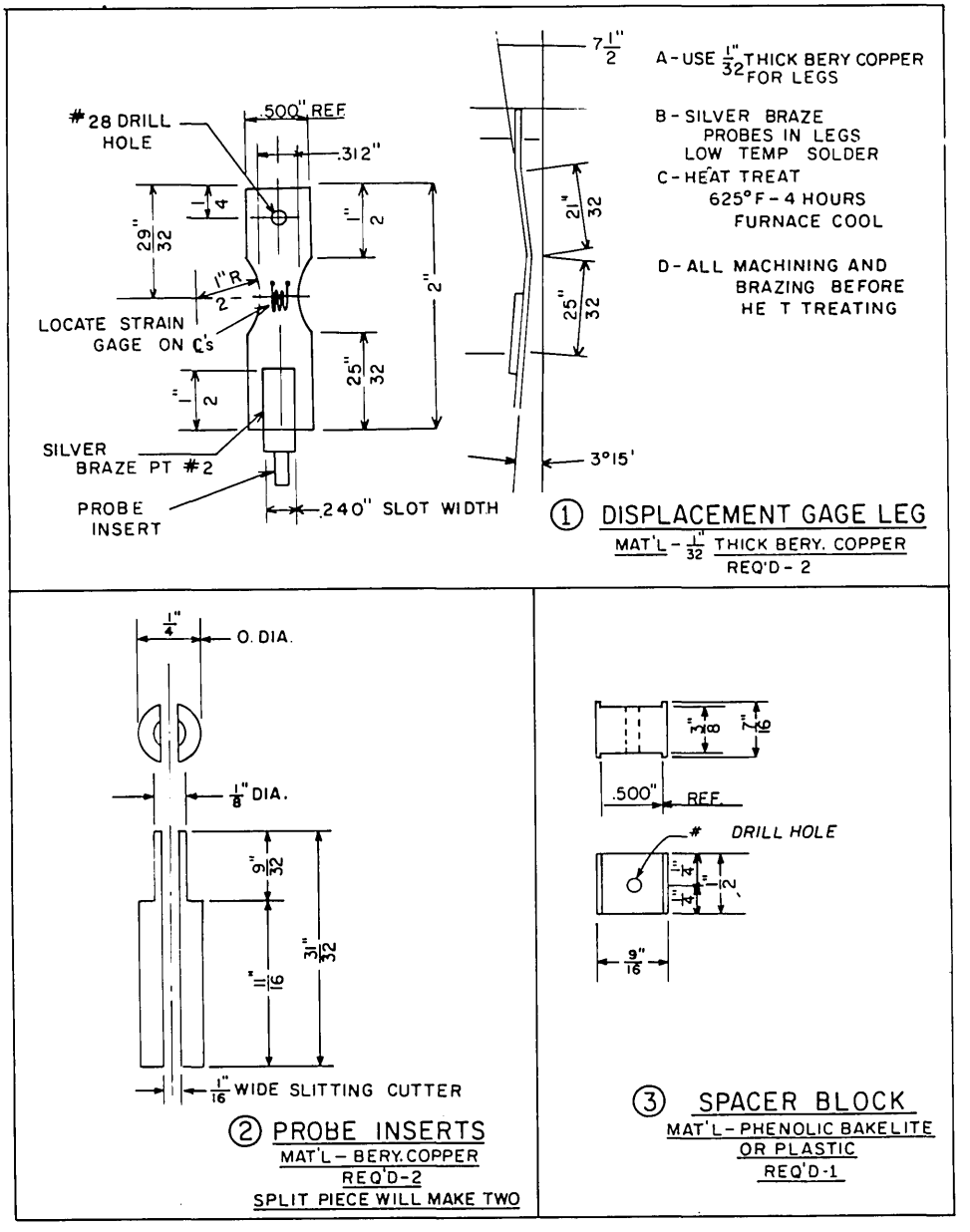

Fig. 11 — Drawing of the probe for center-hole COD measurements

the strain-gage circuit were fed to an XY recorder together with those from the microformer attachment to the load train of a Baldwin Universal Testing Machine.

Since theoretical expressions have been proposed both for displacements at the slit center (16) and at positions quite close to the slit tip (7), it seemed expedient to provide calibration data suitable for comparison. For this reason, a series of calibrations was made positioning the probe at the center of the slit (a_0 from the tip) and at alternate positions 0.3, 0.6, and 1.6 in. from the tip. Tracings of the load P vs COD are shown in Figs. 12a through 12d for these various probe positions. Three runs were made for each determination at a load well below that of instability for this material.

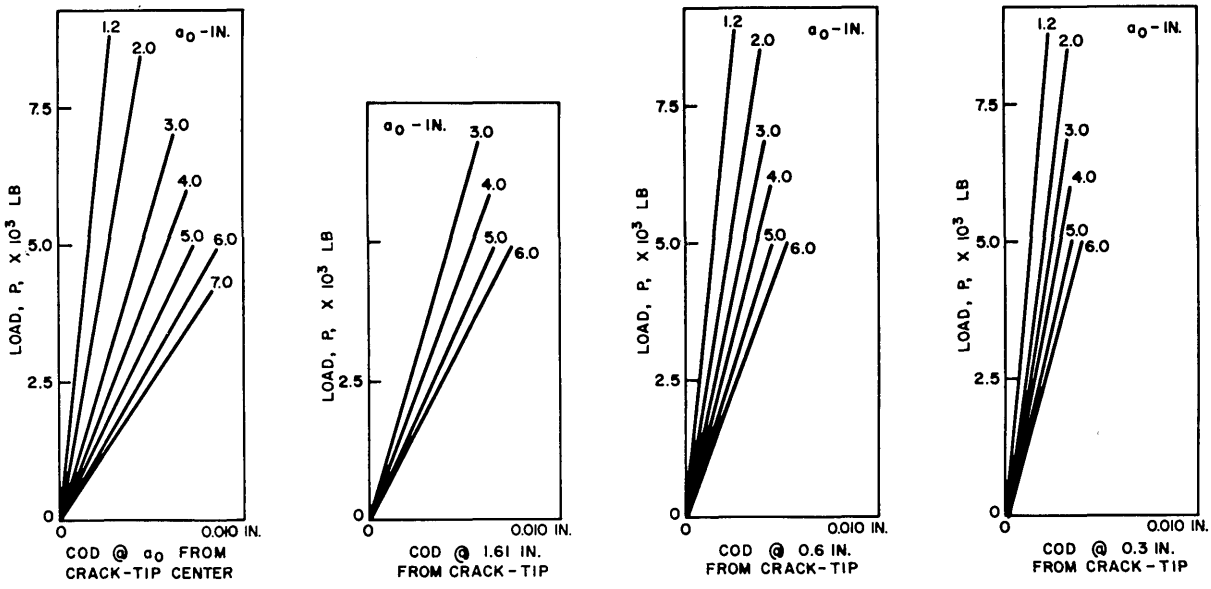

Fig. 12 — Traces of the experimental calibration curves, load vs displacement (P vs COD), for various probe positions. (Ref. 17; Fig. A3)

Data for the center hole position, normalized as $E[COD]/\sigma W = EB[COD]/P$ and plotted against 2a/W, are displayed in Fig. 13. These values are seen to agree well with a theoretical curve plotted from the equation

$$\frac{E[COD]}{\sigma W} = 2\left\{\frac{2W}{\pi Y}\cosh^{-1}\left(\frac{\cosh \pi Y/W}{\cos \pi a/W}\right) - \frac{1+\nu}{\left[1+\left(\frac{\sin \pi a/W}{\sinh \pi Y/W}\right)^2\right]^{1/2}} + \nu\right\} Y/W. \quad (1)$$

Values selected to test the validity of this expression are W = 12 in.; Y= 0.0625 in.; $a = a_0$, the successive half-slit lengths; $\pi = 3.1416$; and $\nu = 0.33$. Substituting these into Eq. (A1) yields

$$\frac{E[COD]}{\sigma W} = 2\left\{122.2\cosh^{-1}\left(\frac{1.0001}{\cos \pi a/W}\right) - \frac{1.33}{\left[1+\left(\frac{\sin \pi a/W}{0.015}\right)^2\right]^{1/2}} + 0.33\right\} 0.0052. \quad (2)$$

Because of the close proximity of the probe to the slit, this calibration is now relatively insensitive to specimen width; computed for width values of W = 3 and 12 in., the plotted curves are indistinguishable. This is not true when Y, the distance of the probe to the slit, is 1 in., a position which has frequently been used (10).

The other positions of the probe are not suitable for length estimates, because as the crack grows, the distance from the crack tip continually increases, thus invalidating the calibration curves. However, they do provide a further check on the experimental method employed by comparison with the theoretical estimate proposed by Irwin (7) and further

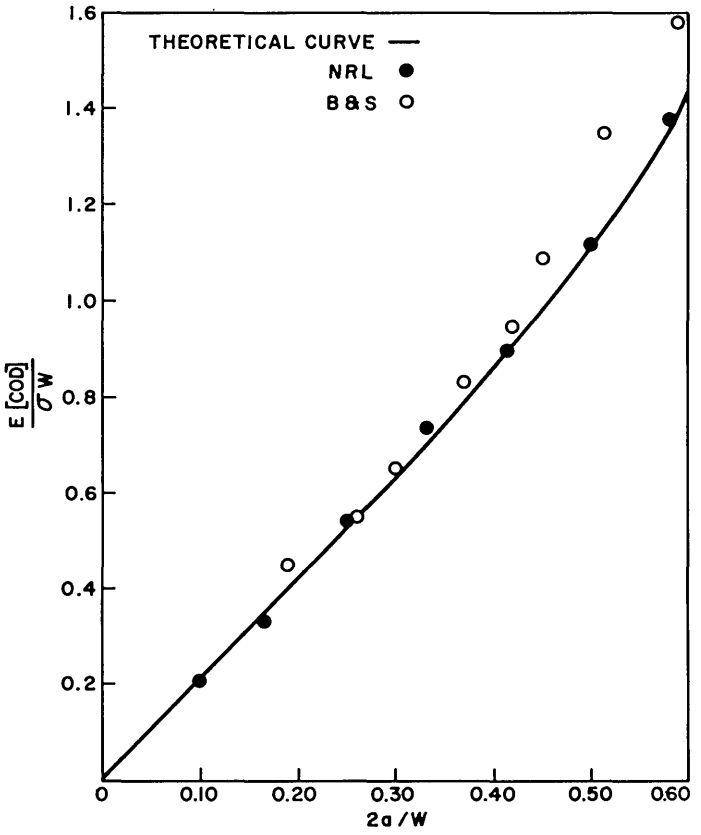

Fig. 13 — Data from Fig. 12 normalized as E[COD]/σW and plotted on the theoretical curve from Eq. 1. (Ref. 17; Fig. A4)

discussed by Paris and Sih (17). Data for all probe hole positions are plotted in Fig. 14 together with theoretical curves from the equation

$$\frac{COD}{2} = \frac{K}{G}(r/2\pi)^{1/2} \sin\frac{\theta}{2}\left[2 - 2\nu - \frac{\cos^2\theta}{2}\right]. \tag{3}$$

Since by definition $K = (P/BW)\sqrt{a}f(2a/W)$ for this center-notched sheet specimen, substitution of K normalizes Eq. (3), giving

$$COD = \frac{(2P/BW)\sqrt{a}f(2a/W)}{G}\left(\frac{r}{2\pi}\right)^{1/2} \sin\frac{\theta}{2}\left[2 - 2\nu - \frac{\cos^2\theta}{2}\right], \tag{4}$$

and

$$\frac{E[COD]}{\sigma W} = \frac{2E}{GW}\sqrt{a}f(2a/W)\left(\frac{r}{2\pi}\right)^{1/2} \sin\frac{\theta}{2}\left[2 - 2\nu - \frac{\cos^2\theta}{2}\right]. \tag{5}$$

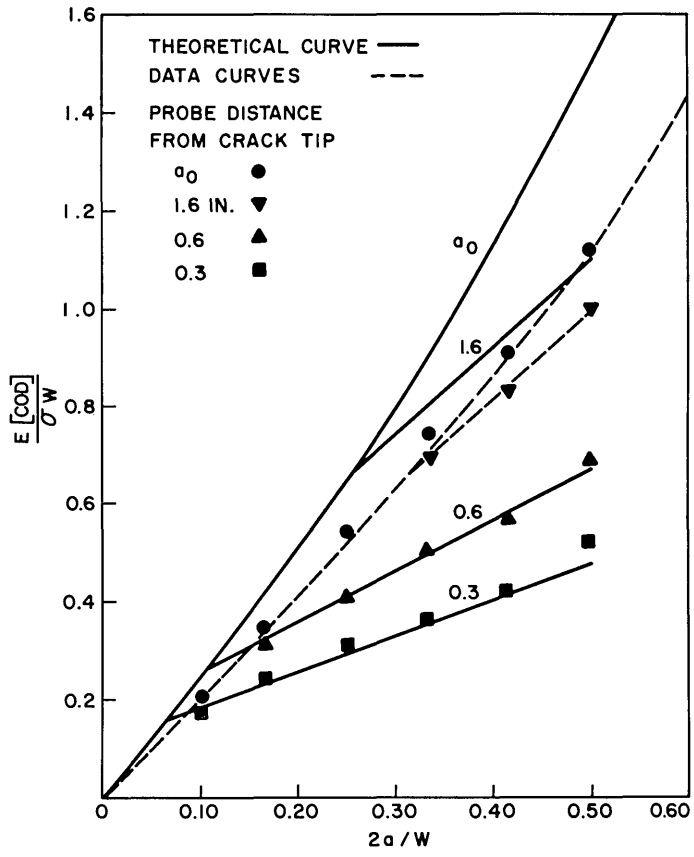

Fig. 14 — All data from Fig. 12 normalized as E[COD]/σW and plotted on the theoretical curves of Eq. 3. (Ref. 17; Fig. A5)

Values selected to test the validity of this expression are W = 12 in.; B = 0.0625 in.; $a = a_0$, the successive half-slit lengths; $\pi = 3.1416$; $\nu = 0.33$; $G = 4.4 \times 10^6$ psi; $E = 10.6 \times 10^6$ psi; $\theta = 180°$; and r = successive positions of the probe from the crack tip. Substituting these values into Eq. (5) yields

$$\frac{E[COD]}{\sigma W} = 0.236 \sqrt{r} \sqrt{a} f(2a/W).$$

The agreement demonstrated for probe positions 0.3 in. and 0.6 in. from the slit tip is surprising, considering that this model was developed to estimate the COD adjacent to the tip.

The comparisons provided in Figs. 13 and 14 serve to ensure confidence in the experimental details (face plates and probe) and the measurement techniques employed. To obtain length estimates of the growing crack, straight lines are drawn from the origin of the load-displacement curve to selected load points. When the slopes are evaluated as COD/P and appropriately normalized (multiply by EB), the value of 2a/W can be read from the calibration curve, and thus crack length can be obtained for known loads. It should be reiterated here that the crack length determined in this manner is considered to be an effective crack length; its use simplifies computation, since the plastic-zone correction need not be added to the basic equation for the evaluation of K.

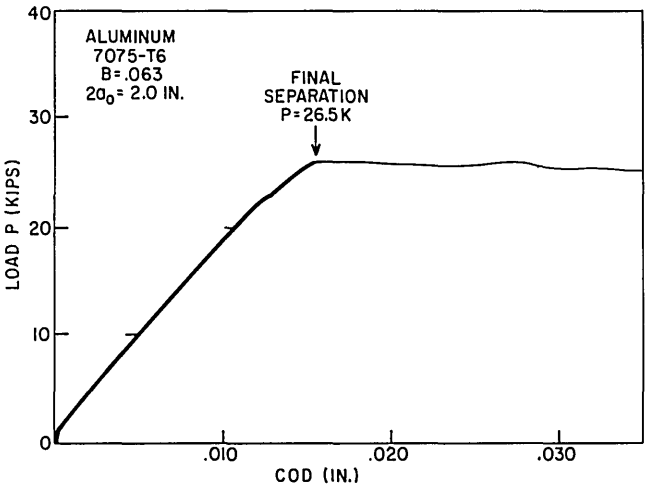

Fig. 15a — Load vs COD for Al 7075-T6

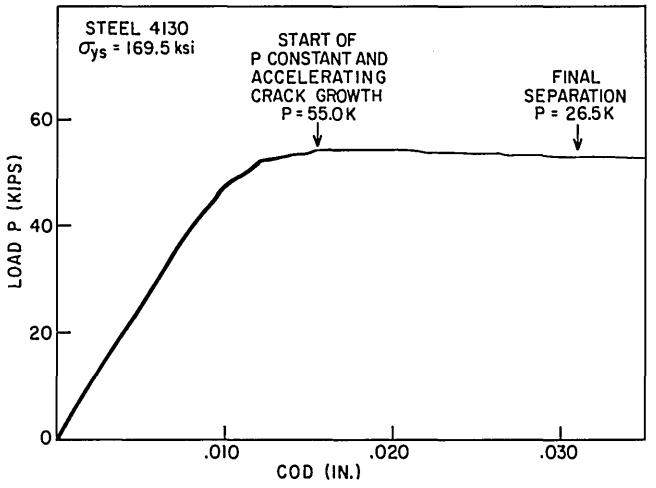

Fig. 15b — Load vs COD for Steel 4130 (σ_{ys} = 169.5 ksi)

Data Reduction

Typical load-COD data curves are shown in Figs. 15a and 15b. To analyze the record:

1. A line is drawn through the best-fit part of the straight-line portion of the curve; this locates the origin and eliminates occasional start-up errors.

2. Straight lines are then drawn from the origin to the loading curve at selected intervals of the COD.

3. The inverse slope COD/P of these lines is now determined. At NRL the lines are drawn with a drafting instrument from which angles can be read; the cotangent of the angle will give the value required when appropriate units are supplied (i.e., multiply by the 45° chart values).

4. This value is then normalized to give EB[COD]/P.

5. The initial crack length being known, the value of EB[COD]/P is read from the calibration curve and compared with the initial crack-length value read from the chart. Frequently small differences will be observed due to shifts in alignment or probe positioning. The difference between the calibration value and the observed value is then added (or subtracted) from all measured values of EB[COD]/P read from the chart.

6. These values are then referred to the calibration curve, and 2a/W values are read off. Simple arithmetic easily gives the crack-length values.

7. Gross stress σ_G is computed for the various load values as load/unnotched area = P/BW.

Since load P and crack length 2a now are known from the test record, K_c is calculated from a modification of the Isida equation (27)

$$K_c = \sigma_G \sqrt{af(2a/W)},$$

where

$$f(2a/W) = 1.77[1 - 0.1(2a/W) + (2a/W)^2].$$

This expression has been found accurate to within 1 percent over the range $0 < 2a/W < 0.6$. This equation is preferred over the commonly used Irwin-Westergard tangent formula since it more properly satisfies the boundary conditions for the specimen. Further polynomial expressions are more convenient for incorporation into data-reduction computer programs.

EXPERIMENTAL PARAMETERS AT OTHER LABORATORIES

A questionnaire was circulated to the following laboratories and individuals:

Alcoa — Kaufman

Armco — McCabe

Battelle — Fedderson

Boeing — Butler

Frankford Arsenal — Carmen

NASA-Langley — Hudson

NRL — Sullivan

North American-Rockwell — Harrigan

Northrup — Wilhem

Reynolds — Zinkham

Spacecraft — Forman

Syracuse — Weiss

This questionnaire and the answers received are provided in the appendix.

DATA ANALYSIS AT NRL

During the past two years over 400 CCT sheet specimens have been tested for the evaluation of K_c. Information and data for the alloys used in these tests — composition, mechanical-property and fracture-resistance data, material source, and heat treatment — are contained in Tables 1, 2, and 3.

Examples of the geometrical dependencies which have been discussed are necessary to comprehend the magnitude of the problem and are now given.

Effect of Specimen Width on K_c

Specimen width will cease to influence K_c if it is "sufficient," i.e., if it can provide constraint by suppressing lateral contraction. The problem is to develop a criterion which will predict the sufficient width necessary for alloys of widely different mechanical and fracture-resistance properties. Insufficient experimentation has been done at this time to set realistic guidelines.

A mathematical development (15,17) indicates that a width equal to $27r_y$ should be sufficient; this hypothesis is illustrated in Fig. 16a. However, in Fig. 16b data are shown for several sheet alloys. For aluminum alloys 7178-T6 and 7075-T6, K_c is unaffected by width W once it has reached $27r_y$. Stainless steel PH 15-7 (WR direction) should be independent by this criterion for specimens over 3 in. wide, yet there is a significant difference between the K_c values of the 12-in.- and 20-in.-wide specimens. (Narrower CCT specimens have yet to be tested.) The 20-in.-wide specimen may, however, represent an unexplained anomaly, since Armco Research Laboratory (36) reports constant K_c values for 5-in.- and 10-in.-wide crack-lined-loaded (CLL) specimens which correspond to 10-in. and 20-in. CCT specimens.

Effect of Crack-Length-to-Width Ratio

The dependency of the crack-length-to-width ratio 2a/W is shown in Fig. 17. From these data it has been concluded that if 2a/W at instability is greater than 0.10 and less than 0.50, the K_c value will be unaffected, a scatterband of ± 10 percent being reasonable.

Effect of Sheet Thickness

Figure 18 illustrates the anticipated dependency of K_c on specimen thickness B. It seemed plausible that at some sheet thickness, specific for each alloy, a maximum K_c value would be obtained and that it would be accompanied by 100-percent slant fracture. Thereafter, as the thickness continued to increase and increasing amounts of flat fracture were noted, K_c would decrease to the minimum value of K_{Ic} at 100-percent flat fracture.

How closely this anticipated behavior is achieved in real materials is illustrated in Fig. 19 for aluminum alloys and in Fig. 20 for titanium alloys. The accompanying plots indicate the percent of slant fracture observed. Solid curves are shown in conformity with a model (37) purporting to explain the thickness-dependency effects; these curves indicate that this model is not satisfactory for these data.

Table 1
Properties of Aluminum Alloys

Aluminum Alloy*	Sheet Thickness (in.)	Yield Strength 0.2% Offset (ksi)	Tensile Strength (ksi)	Elongation (%)	Reduction in Area (in.^{2})	K_c Blunt (ksi $\sqrt{in.}$)	K_c Sharp (ksi $\sqrt{in.}$)
7178-T6							
Kaiser I	0.032	77.0	87.5	9.2	23.2	61.5	—
Kaiser II	0.040	79.2	89.7	9.5	13.7	47.3	49.4
Kaiser I	0.063	78.9	88.7	9.8	20.5	55.4	50.2
Alcoa II	0.091	77.8	88.4	11.0	20.8	44.7	44.6
Reynolds II	0.127	77.0	89.6	12.0	19.4	51.6	45.4
7079-T6							
Reynolds	0.037	68.8	78.5	9.0	13.7	62.2	62.0
Reynolds	0.060	71.1	78.6	9.7	18.6	73.0	70.8
Reynolds	0.100	62.4	73.7	12.2	23.0	95.3	98.6
Reynolds	0.136	71.8	81.4	11.0	2.2	69.1	68.6
—	0.25	65.9	76.2	11.0	25.1	78.0	80.6
7075-T6							
Alcoa II	0.032	70.9	80.6	9.7	19.7	63.9	51.5
Alcoa I	0.063	—	—	—	—	65.2	—
Alcan II	0.063	76.5	88.5	10.8	22.8	61.2	61.0
Alcan I	0.090	—	—	—	—	70.2	—
Alcoa II	0.093	74.2	82.4	8.9	19.6	73.2	65.1
Alcoa I	0.100	—	—	—	—	58.1	—
Alcan II	0.102	75.0	84.4	8.9	21.4	57.9	62.4
Alcan I	0.125	—	—	—	—	57.1	—
Alcan II	0.126	75.8	85.7	10.7	21.2	52.8	54.4
Alcan II	0.198	75.6	86.6	9.5	13.7	53.0	56.8
—	0.250	73.6	84.1	9.5	17.0	49.5	46.1
2014-T6							
Alcoa	0.040 (Alclad)	61.5	68.1	7.7	15.8	82.0	75.2
—	0.063 (Bare)	61.2	69.1	9.0	17.3	72.2	72.1
Reynolds	0.090 (Alclad)	57.4	69.0	11.2	23.1	74.5	75.2
Alcoa	0.125 (Alclad)	59.6	67.4	9.7	19.1	86.8	92.1
Alcan	0.25 (Alclad)	59.3	66.8	8.5	17.3	68.5	65.9
2024-T3							
Kaiser	0.063	46.1	68.6	16.0	20.7	97.0	—
Olin	0.125	49.3	70.9	17.5	23.5	102.0	—
Olin	0.188	47.6	70.1	17.5	18.6	106.4	—
Reynolds	0.250	45.1	68.3	17.0	20.8	96.0	—

*Fracture direction: WR

Table 2
Properties of Titanium Alloys

Titanium Alloy*	Sheet Thickness (in.)	Yield Strength 0.2% Offset (ksi)	Tensile Strength (ksi)	Elongation (%)	Reduction in Area (%)	K_c Blunt (ksi $\sqrt{in.}$)	K_c Sharp (ksi $\sqrt{in.}$)	Heat Treatment
6Al-4V	0.032	—	135.9	—	—	51.5	53.5	Solution anneal: 1780°F, 20 min; water-spray quench; age: 975°F, 8 hr; air cool
	0.063	151.1	156.3	1.0	2.0	74.4	64.2	
	0.090	158.5	168.9	3.0	—	97.6	77.5	
	0.125	146.0	158.2	4.2	7.5	90.4	—	
4Al-3Mo-1V	0.042	161.5	167.0	0.5	0.3	—	50.2	Solution anneal: 1650°F, 15 min; water-spray quench; age: 925°F, 14 hr; air cool
	0.058	153.4	174.5	0.75	1.8	—	54.8	
	0.087	152.9	172.0	0.5	1.1	64.0	62.5	
	0.124	159.8	172.1	1.0	1.0	64.5	35.0	
16V-2.5Al	0.041	181.6	190.5	1.5	3.9	56.6	52.4	Solution anneal: 1380°F, 15 min; water-spray quench; age: 960°F, 4 hr; air cool
	0.059	176.5	187.6	4.7	9.5	65.2	46.3	
	0.118	181.7	192.0	4.0	9.5	51.2	44.4	
13V-11Cr-3Al	0.040	198.1	199.4	0.0	2.9	55.8	34.1	Age: 900°F, 72 hr; air cool
	0.063	207.3	220.9	2.7	6.3	41.5	38.9	
	0.090	200.6	203.5	0.0	—	52.6	29.8	
	0.125	216.5	227.0	2.2	2.1	35.7	23.2	

*Fraction direction: WR

Table 3
Properties of Steel Alloys

Steel	Sheet Thickness (in.)	Yield Strength 0.2% Offset (ksi)	Tensile Strength (ksi)	Elongation (%)	Reduction in Area (%)	Fracture Direction	K_c Blunt (ksi $\sqrt{in.}$)	K_c Sharp (ksi $\sqrt{in.}$)	Heat Treatment
4130	0.063	169.5	192.5	3.9	11.3	WR	160.0	171.9	Austenitize: 1575°F, 1 hr; water-spray quench; Temper: 700°F, 30 min; air cool
4130	0.063	178.4	225.1	5.3	27.8	WR	140.8	137.5	Austenitize: 1575°F, 1/2 hr; water-spray quench; Temper: 500°F 30 min; air cool
15-7*	0.05	212.0	—	—	—	WR	112.5	—	Heat: 1750°F, 10 min; Cool: in air to room temperature; —100°F, 8 hr Reheat: 1050°F, 1 hr
	0.05	219.1	229.4	—	—	RW	—	—	

*Donated and heat treated by Armco

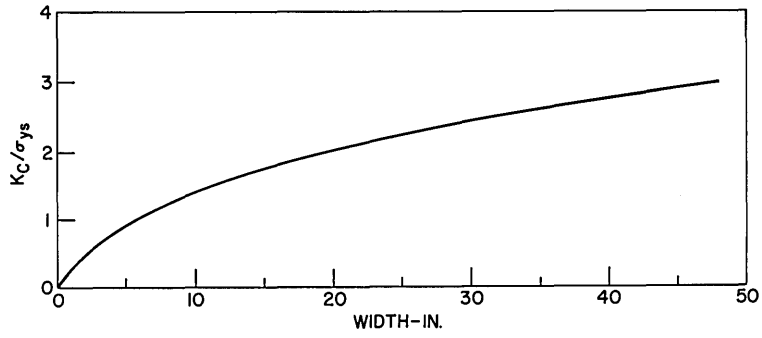

Fig. 16a — Postulated relationship of K_c/σ_{ys} vs W = 27 r_y. (Ref. 23; Fig. 2)

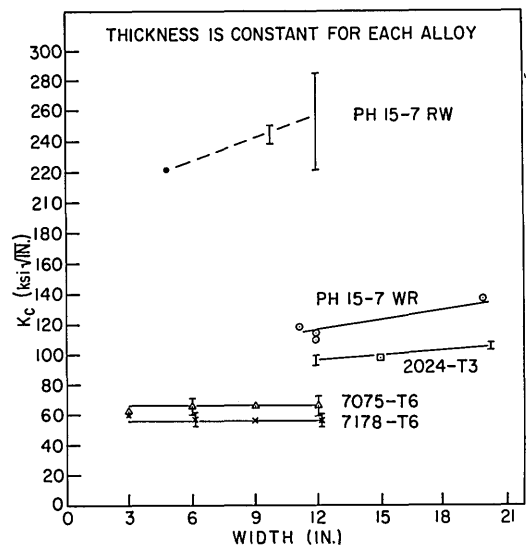

Fig. 16b — K_c vs W for four alloys. The thickness is constant for each alloy.

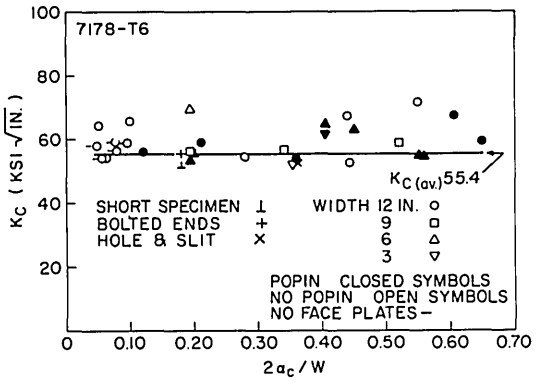

(a) Al 7178-T6 (Ref. 17; Fig. 2)

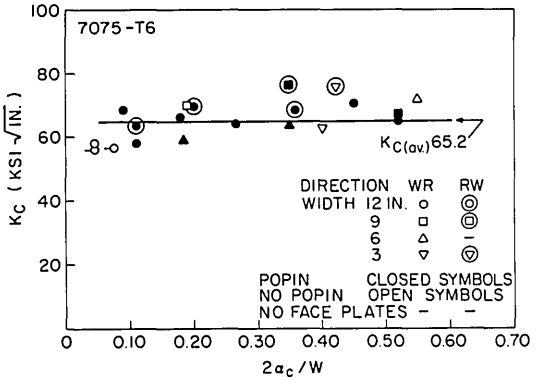

(b) Al 7075-T6 (Ref. 17; Fig. 3)

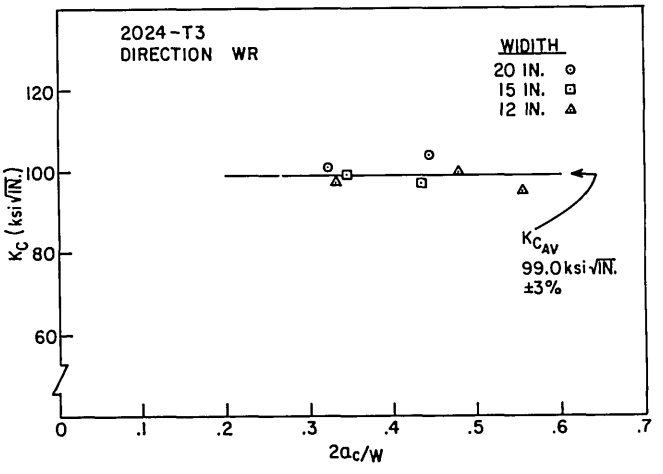

(c) Al 2024-T3

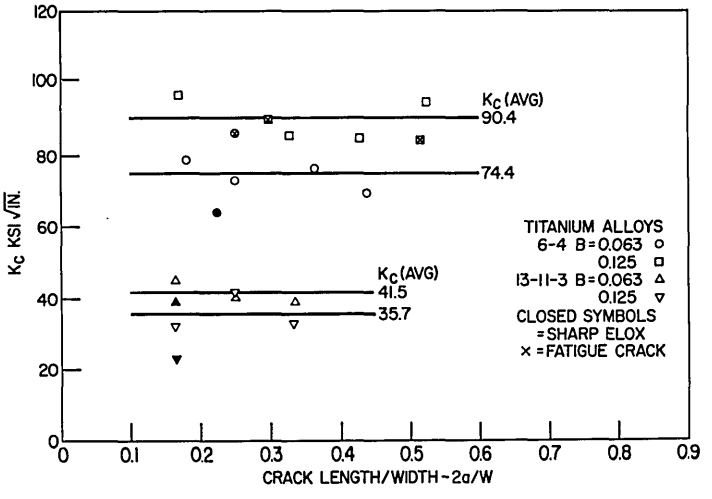

(d) Ti 6-4 and 13-11-3 (Ref. 23; Fig. 3)

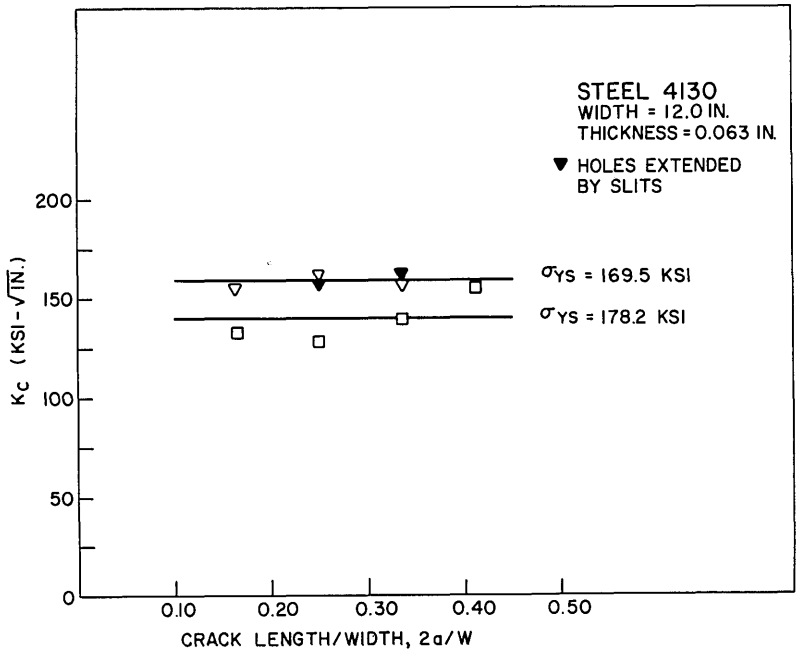

(e) Steel 4130 (Ref. 19; Fig. 3)

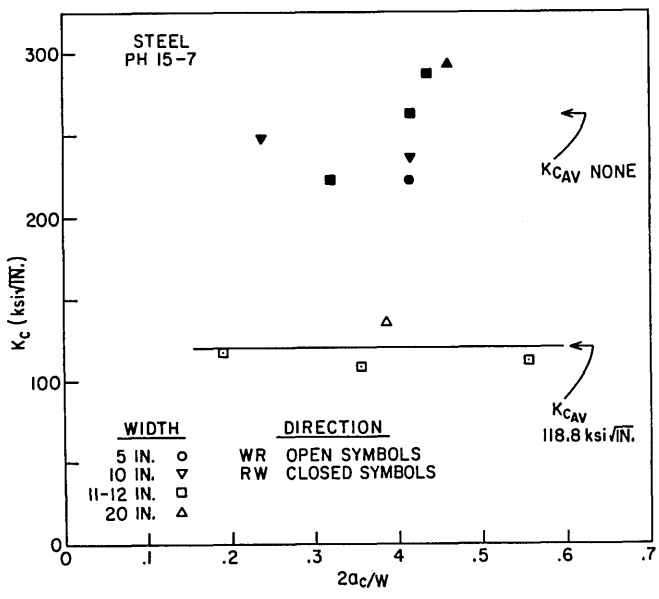

(f) Steel PH 15-7

Fig. 17 — Relationship between K_c and crack-length-to-width ratio 2a/W for various alloys

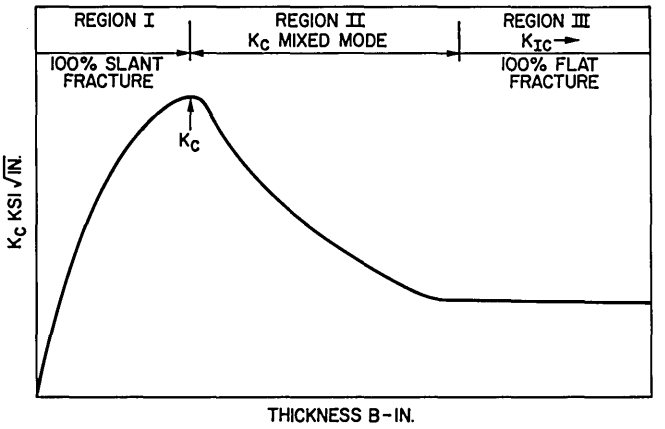

Fig. 18 — Relationship between K_c and sheet thickness B (Ref. 23; Fig. 4)

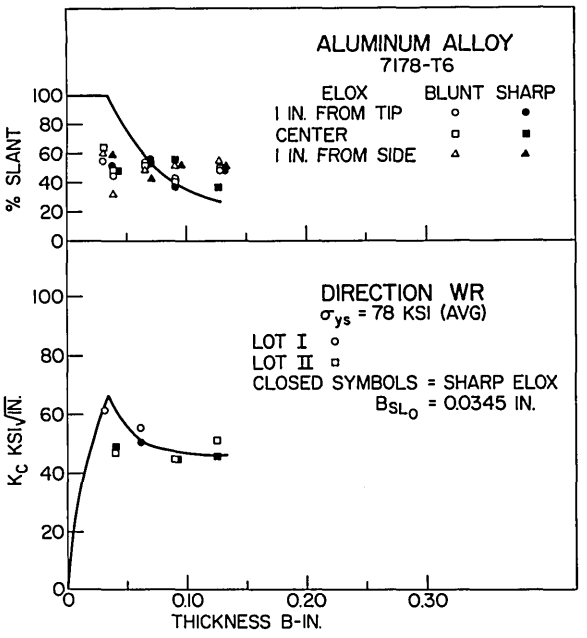

(a) 7178-T6 (Ref. 24; Fig. 2a)

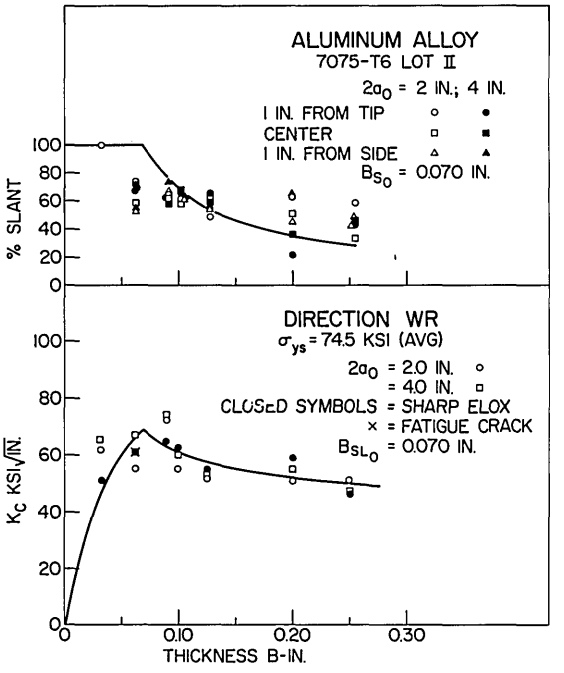

(b) 7075-T6 (Ref. 24; Fig. 2b)

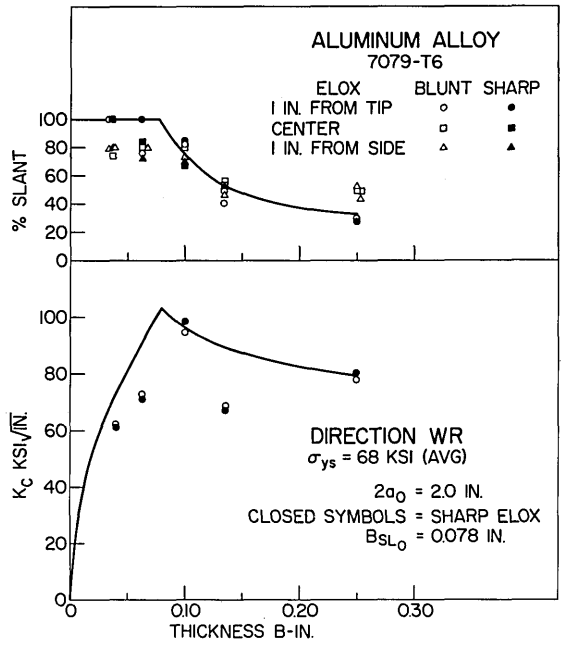

(c) 7079-T6 (Ref. 24; Fig. 2c)

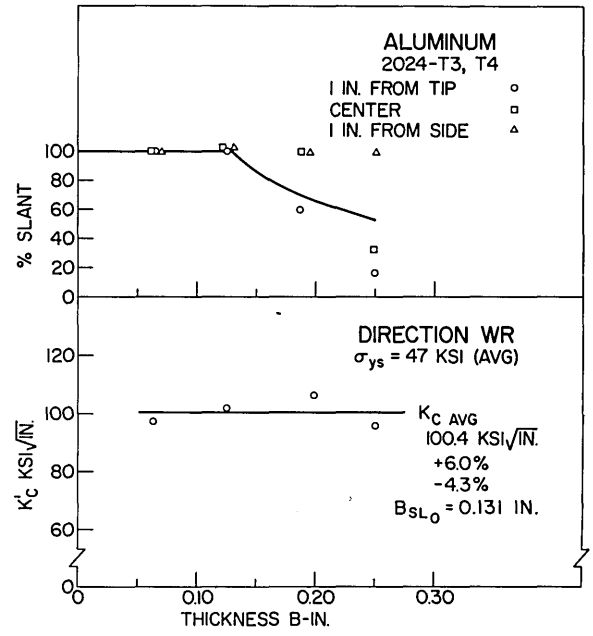

(d) 2024-T3, T4 (Ref. 24; Fig. 2d)

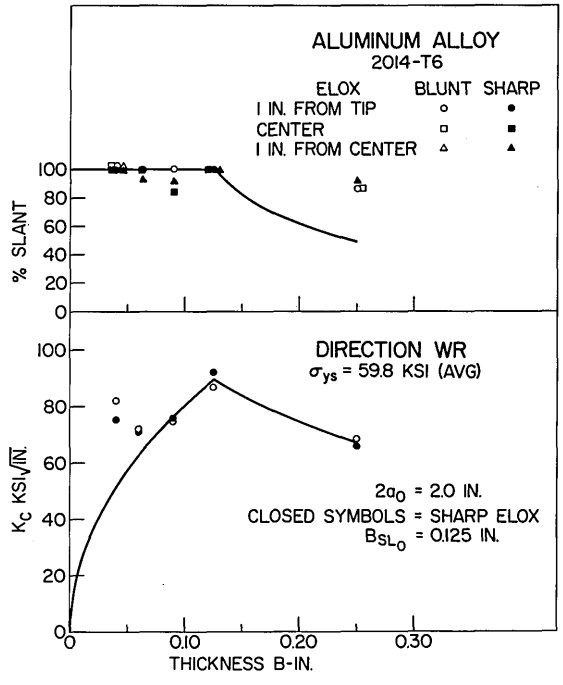

(e) 2014-T6 (Ref. 24; Fig. 2e)

Fig. 19 — K_c and percent slant fracture vs sheet thickness for aluminum alloys

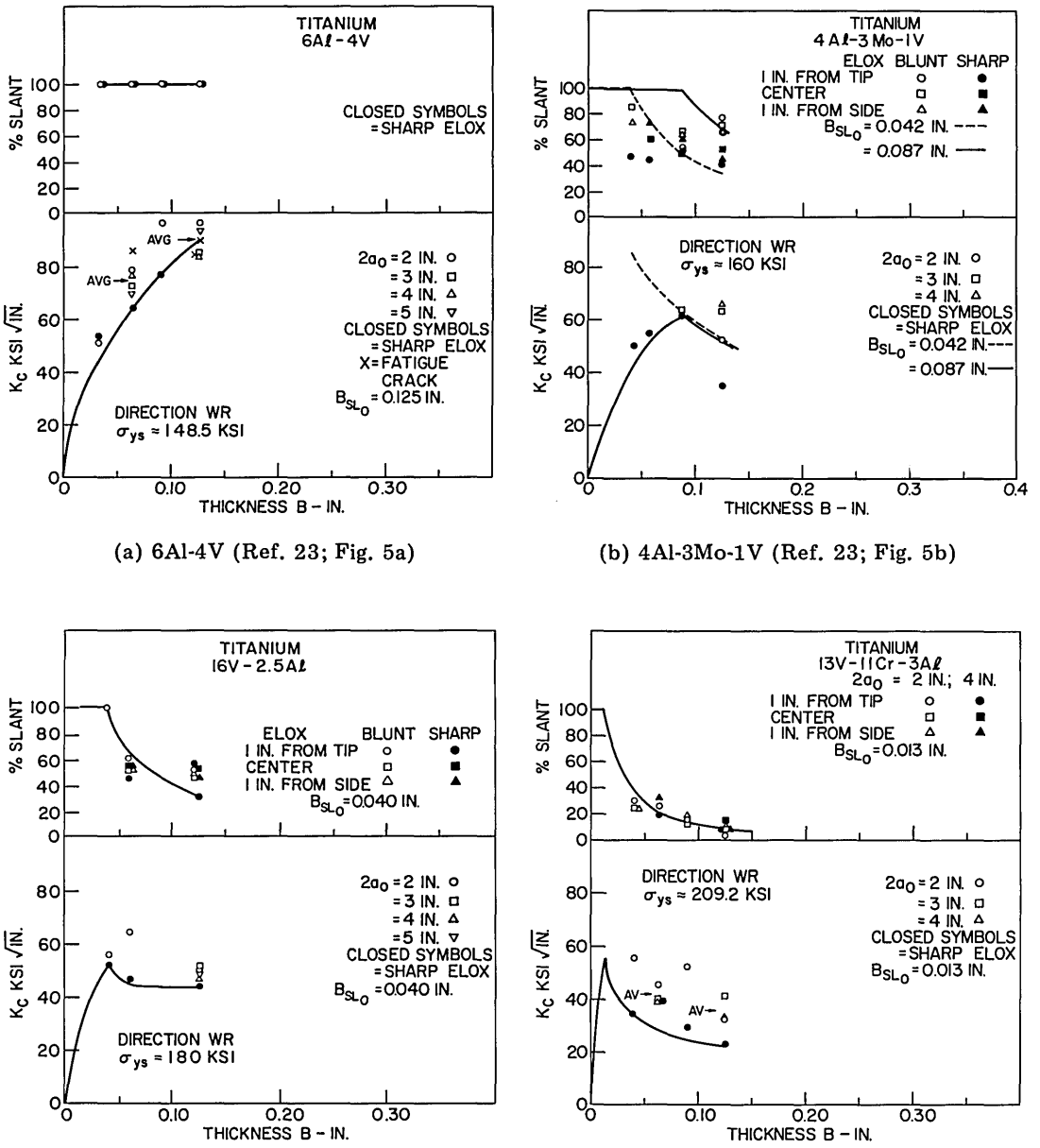

(a) 6Al-4V (Ref. 23; Fig. 5a)

(b) 4Al-3Mo-1V (Ref. 23; Fig. 5b)

(c) 16V-2.5Al (Ref. 23; Fig. 5c)

(d) 13V-11Cr-3Al (Ref. 23; Fig. 5d)

Fig. 20 — K_c and percent slant fracture vs sheet thickness for titanium alloys

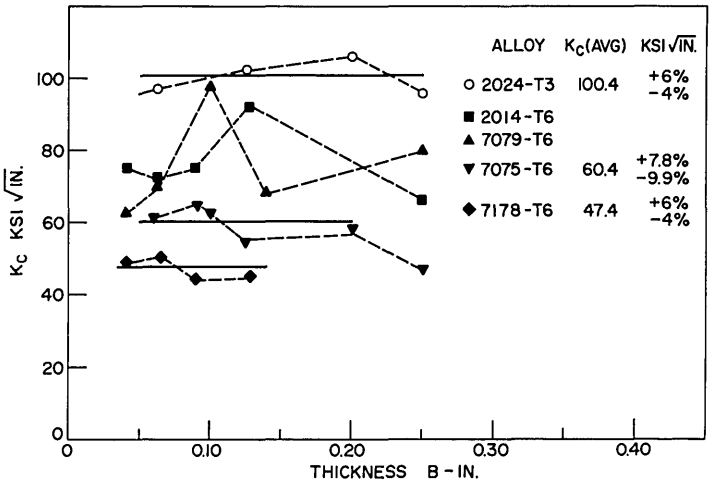

Fig. 21 — Composite K_c vs B for the aluminum alloys

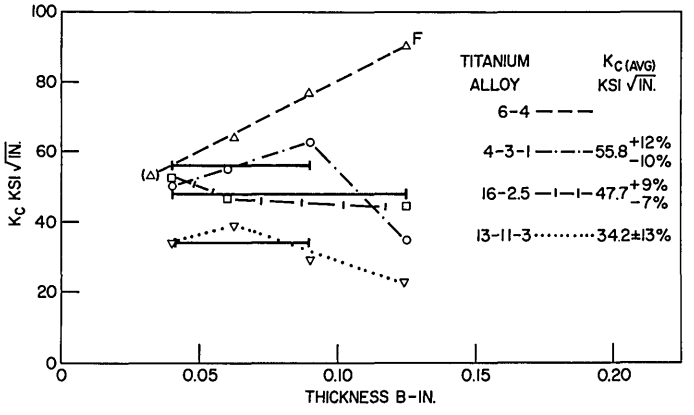

Fig. 22 — Composite K_c vs B for the titanium alloys (Ref. 23; Fig. 7)

Further, in Figs. 21 and 22 it is seen that for three each of the aluminum- and titanium-alloy series, K_c is essentially constant over the thickness range of 0.03 to 0.125 in.

Effect of Notch Root Radius on K_c

Two notch tip configurations have been used at NRL. A blunt tip with a radius typically 3 to 6 mils was Eloxed in all specimens; in selected panels the original slit was extended to develop a 1-mil radius.

It has been shown (7,28) that if slow stable crack growth precedes instability, blunt slits will provide less stress concentration than a sharp crack, and this causes K_c to be overestimated.

In Fig. 23, panels containing sharp tips produced slightly lower K_c values for any thickness than did those with blunt tips. For Ti-13V-11Cr-3Al, no slow stable growth

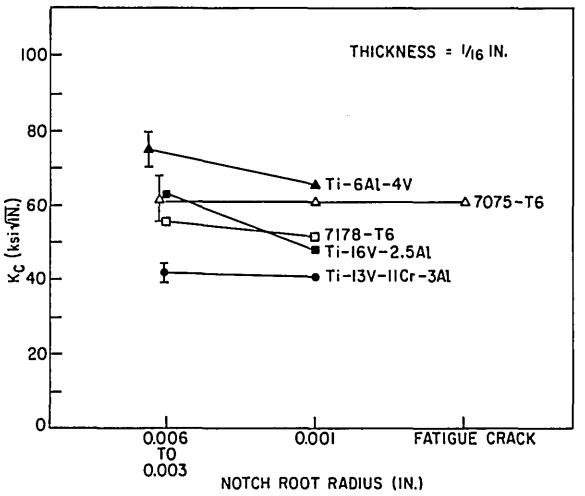

Fig. 23 — K_c vs notch root radius

was observed, and the slightly lower K_c for the sharp-tip specimen is expected. The aluminum alloys and Ti-6Al-4V manifested stable crack extension prior to instability for both blunt- and sharp-tip specimens; though 7075-T6 did not indicate sensitivity, 7178-T6 and Ti-6Al-4V seemed to be influenced by the initial tip radius. the Ti-16V-2.5Al evidenced crack growth from the sharp tip but no growth from the blunt tip, so K_c would be expected to be influenced by the tip radius, as in Ti-13V-11Cr-3Al.

The mixed results indicated in Fig. 23 may be due to the influence of variations in melting and processing practice and a small difference in alloy chemistry.

Definition of Instability

Examination of load-vs-crack-growth records for materials studied here has shown two types of crack-extension behavior, which are illustrated in Fig. 24. The upper boundary of Region I defines the load required to initiate growth at the crack tip; in Region II the crack propagates under a continually rising load. If the load is held constant in this region, growth ceases. For the more brittle alloys, propagation under the rising load continues until the combination of load and crack length becomes critical, at which unstable fracture ensues.

Though tougher alloys also exhibit Region I and Region II behavior, final separation does not occur at the end of Region II. Instead, at this point the load remains constant while the crack grows at an accelerating rate; this type of growth is designated as Region III. Noted previously by Broek (38) and Campbell (39), it was suggested that the K level at commencement of Region III and the K level at final specimen separation are relevant damage criteria. However, Srawley and Brown (29) define instability as occurring at the maximum load value, the inflection point of load vs crack extension of zero slope, e.g., $dP/d2a = 0$. Practically, it seems reasonable that the start of Region III behavior (crack growth under constant load) marks the limit of structural integrity. Therefore, the crack length at this position, the start of Region III, is used to calculate K_c for materials exhibiting such behavior.

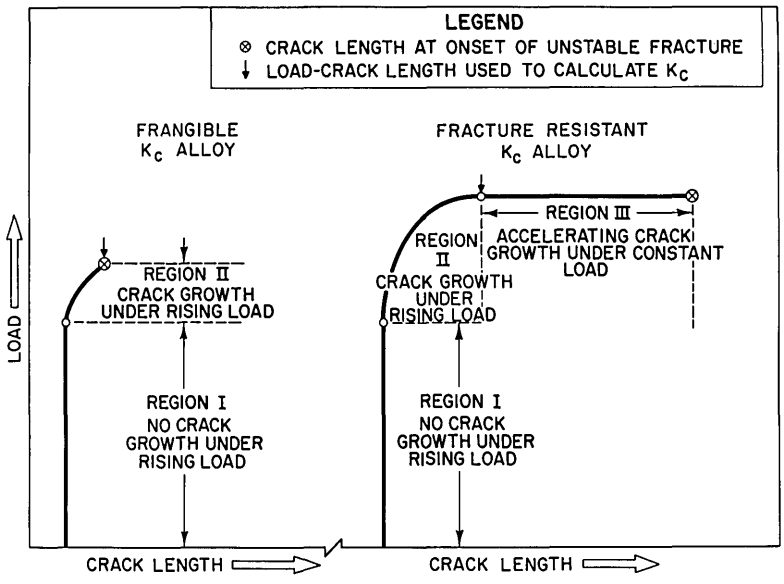

Fig. 24 — Two types of crack-growth behavior (Ref. 18; Fig. 5)

CONCLUSIONS

The renewed interest in K_c testing is now producing a large quantity of data. This situation is expected to continue for some time, as there are still many unanswered questions. There does not seem to be any general uniformity of practice for CCT testing (by inspection of the relatively few returns to the questionnaire circulated). This is unfortunate, as it prevents significant comparisons. However, this is understandable, since a standard recommended practice is now only in the earliest stage of formulation.

The experience gained in K_{Ic} testing has resulted in a clearer understanding of the fracture-resistance parameter and the nature of the problems involved in determining it. Further, compared to the rather primitive testing procedures employed earlier, current procedures, although somewhat diverse, display marked sophistication and ingenuity.

RECOMMENDATIONS

Further attention should be given to the following aspects of thin-sheet fracture-toughness testing using the CCT specimen:

- Effect of specimen length
- Effect of specimen width
- Effect of specimen thickness
- Effect of crack tip radius
- Definition of instability, i.e., load and crack length to be used for calculation
- Influence of a_0 on a_c

- Effect of variations in chemistry and processing; i.e., when studying any one of the above and for any round-robin tests, (a) all material should be from the same lot for a particular series of tests and (b) where possible the same material from several different sources should be tested.

REFERENCES

1. *Fracture Toughness Testing and Its Application*, ASTM STP 381, 1965.
2. J.G. Kaufman and A.H. Knoll, "Kahn-Type Tear Tests and Crack Toughness of Aluminum Alloy Sheet," *Materials Res. and Stds.* 4, 151 (1964).
3. D. Broek, "The Residual Strength of Cracked Sheet-Tests Interrupted After Intermediate Slow Crack Growth," National Aerospace Laboratory (Amsterdam) Technical Report No. NLR-TR M.2145, July 1965.
4. D. Broek and F.A. Jacobs, "The Static Strength of Aluminium Alloy Sheet Specimens Containing Blunt Notches," National Aerospace Laboratory (Amsterdam) Technical Report No. NLR-TR M.2149, Aug. 1965.
5. D. Broek and A. Nederveen, "The Influence of the Loading Rate on the Residual Strength of Aluminium Alloy Sheet Specimens," National Aerospace Laboratory (Amsterdam) Technical Report No. NLR-TR M.2154, Oct. 1965.
6. D. Broek, "The Effect of the Sheet Thickness on the Fracture Toughness of Cracked Sheet," National Aerospace Laboratory (Amsterdam) Technical Report No. NLR-TR M.2160, Jan. 1966.
7. D. Broek, "The Residual Strength of Aluminium Alloy Sheet Specimens Containing Fatigue Cracks or Saw Cuts," National Aerospace Laboratory (Amsterdam) Technical Report NLR-TR M.2143, Mar. 1966.
8. D. Broek, "Static Tests on Cracked Panels of 2024-T3 Alclad Sheet Materials from Different Manufacturers," National Aerospace Laboratory (Amsterdam) Technical Report No. NLR-TN M.2164, Nov. 1966.
9. C.M. Carman, D.F. Armiento, and H. Marcus, "Crack Resistance Properties of High Strength Aluminum Alloys," in *Proceedings of First International Conference on Fracture* (Sendai, Japan) Vol. 2, 1966, p. 995.
10. C.M. Carman and G.R. Irwin, "Plane Stress Fracture Toughness Testing," Note for ASTM Committee E-24 Meeting, Cleveland, Ohio, Oct. 1969.
11. C.M. Carman and G.R. Irwin, "Relation of Crack Opening Stretch and Thickness Contraction to R Curves for Evaluating Fracture Toughness," Frankford Arsenal Report R-2029, Dec. 1971.
12. R.G. Forman, "Experimental Program to Determine Effect of Crack Buckling and Specimen Dimensions on Fracture Toughness of Thin Sheet Materials," AF Flight Dynamics Laboratory Technical Report AFFDL-TR-65-146, Wright-Patterson AFB, Ohio, 1966.
13. *Damage Tolerance in Aircraft Structures*, ASTM STP 486, 1971.
14. F.C. Allen, "Effect of Thickness on the Fracture Toughness of 7075 Aluminum in the T6 and T73 Conditions," ASTM STP 486, 1971, p. 16.

15. C.E. Feddersen, "Evaluation and Prediction of the Residual Strength of Center Cracked Tension Panels," ASTM STP 486, 1971, p. 50.

16. T. Swift, "Development of the Fail-Safe Design Features of the DC-10," ASTM STP 486, 1971, p. 164.

17. A.M. Sullivan and C.N. Freed, "The Influence of Geometric Variables on K_c Values for Two Thin Sheet Aluminum Alloys," NRL Report 7270, June 17, 1971.

18. C.N. Freed, A.M. Sullivan, and J. Stoop, "Comparison of Plane-Stress Fracture Toughness for Three Aluminum Sheet Alloys," NRL Report 7299, Aug. 11, 1971.

19. A.M. Sullivan and C.N. Freed, "Plane Stress Fracture Resistance of One Steel Sheet and Two Titanium Sheet Alloys," NRL Report 7332, Oct. 27, 1971.

20. C.N. Freed, A.M. Sullivan, and J. Stoop, "Crack-Growth Resistance Characteristics of High-Strength Sheet Alloys," NRL Report 7374, Jan. 31, 1972.

21. C.N. Freed, A.M. Sullivan, and J. Stoop, "Influence of Dimensions of Center-Cracked Tension Specimen on K_c," Presented at the Fifth National Symposium on Fracture Mechanics, Urbana, Illinois, Sept. 1971 (pending publication in ASTM STP).

22. A.M. Sullivan, C.N. Freed, and J. Stoop, "A Comparison of R Curves Determined from Different Specimen Types," Presented at R-Curve Technical Session, ASTM Committee E-24 Meeting, Hawthorne, California, Oct. 1971 (pending publication by ASTM).

23. A.M. Sullivan, J. Stoop, and C.N. Freed, "Plane Stress Fracture Resistance of High Strength Titanium Alloy Sheet," Second International Conference on Titanium, Boston, Mass., May 1972 (pending publication in Conference Proceedings).

24. A.M. Sullivan, J. Stoop, and C.N. Freed, "The Influence of Sheet Thickness Upon the Fracture Resistance of Structural Aluminum Alloys," submitted for the Sixth National Symposium on Fracture Mechanics, Philadelphia, Penn., Aug. 1972.

25. F.A. McClintock and G.R. Irwin, "Plasticity Aspects of Fracture Mechanics," ASTM STP 381, 1965.

26. P.C. Paris and G.C. Sih, "Stress Analysis of Cracks," in *Fracture Toughness Testing and Its Applications*, ASTM STP 381, 1965, p. 30.

27. W.F. Brown, Jr., and J.E. Srawley, "Plane Strain Crack Toughness Testing of High Strength Metallic Materials," ASTM STP 410, 1966.

28. F.J. Bradshaw, D. Lacey, and C. Wheeler, "The Effect of Section Thickness on the Crack Resistance of Aluminum L93, with Measurements of Plastic Strain," Royal Aircraft Establishment (U.K.) Technical Report 72039.

29. J.E. Srawley and W.F. Brown, Jr., "Fracture Toughness Testing Methods," in *Fracture Toughness Testing and Its Applications*," ASTM STP 381, 1965, p. 133.

30. G.R. Irwin, "Fracture Dynamics," in *Fracturing of Metals*, ASM, Cleveland, 1948, p. 147.

31. "Fracture Testing of High-Strength Sheet Materials: A Report of a Special ASTM Committee," ASTM Bulletin, No. 243, 29-40 and No. 244, 18-28, Jan. and Feb. 1960.

32. Special ASTM Committee on Fracture Testing of High-Strength Materials, "Progress in Measuring Fracture Toughness and Using Fracture Mechanics," in *Materials Res. and Stds.* Vol. 4, No. 3, Mar. 1964, p. 107.

33. M.H. Jones and W.F. Brown, Jr., "Acoustic Detection of Crack Initiation in Sharply Notched Specimens," in *Materials Res. and Stds.*, Vol. 4, No. 3, 1964, p. 120.

34. R.W. Boyle, "A Method for Determining Crack Growth in Notched Sheet Specimens," in *Materials Res. and Stds.*, Vol. 2, No. 8, 1962, p. 646.

35. J.E. Srawley, M.H. Jones, and B. Gross, "Experimental Determination of the Dependence of Crack Extension Force on Crack Length for a Single Edge Notched Tensile Specimen," NASA TN D2396, Aug. 1964.

36. R.H. Heyer and D.E. McCabe, "Plane Stress Fracture Toughness Using a Crack-Line-Loaded Specimen," Third National Symposium on Fracture Mechanics, Bethlehem, Penn., Aug. 1969, to be published in *J. of Eng. Fracture Mechanics.*

37. J.I. Bluhm, "A Model for the Effect of Thickness on Fracture Toughness," Proc. ASTM 61, 1324 (1961).

38. D. Broek, "The Residual Strength of Light Alloy Sheets Containing Fatigue Cracks," in *Aerospace Proceedings*, 1966, p. 811.

39. J.E. Campbell, "Mechanical Properties of Metals," Defense Materials Information Center Review, Jan. 15, 1971.

APPENDIX

QUESTIONNAIRE AND ANSWERS

The following questionnaire was circulated. The answers have been reduced to the same tabular format and are included. When information was gathered from a report rather than from the questionnaire, this is cited.

Questionnaire

Center-Cracked Tensile Specimens Experimental Parameters

1. Test Specimen
   a. Width W
   b. Length L
   c. Crack length 2a
   d. Thickness B

2. Notch Preparation
   a. Size and shape
   b. How inserted?
   c. Fatigued?

3. Buckling Restraint
   a. Type
   b. When used? (i.e., thickness where considered necessary)

4. Load and Crack-Length Measurement
   a. Load
   b. Crack-length measurement

5. Data Reduction
   a. Equation used
   b. Plastic-zone correction?
   c. Values of load and crack length used to compute K_c specifically
      (1) Load P and crack length 2a at instability: P_c and 2_{ac}
      (2) Load max. and initial crack length: P_m and 2_a
      (3) ?

AIR FORCE FLIGHT DYNAMICS LABORATORY

Wright-Patterson Air Force Base

"Experimental Program to Determine the Effect of Crack Buckling and Specimen Dimensions on Fracture Toughness of Thin Sheet Materials"

R.G. Forman Technical Report AFFDL-TR-65-146 January 1966

1. SPECIMEN

a. Width	W (in.)	7, 8, 10, 12, 16, 20, 22, 24, 48
b. Length	L (in.)	1.6; 1.8; 3.2; 3.65; 5.65; 5.8; 10.2; 15; 39
c. Crack length	(in.)	Varied
d. Thickness	B (in.)	0.02; 0.06; 0.063

2. NOTCH PREPARATION

a. Size and shape	No information
b. How inserted	No information
c. Fatigued	No

3. BUCKLING RESTRAINT

a. Type	Metal plates front and rear with slot to observe crack
b. When used	To measure effect of buckling on $\mathcal{G}_c$

4. LOAD AND CRACK-LENGTH MEASUREMENT

a. Load	Recorded at crack-length stops
b. Crack length	Grid lines 0.1 in. apart on specimen when line reached, loading stopped and crack length estimated to nearest 0.03 in.

5. DATA REDUCTION

a. Equation	$\mathcal{G}_c$ = Not given α = Width correction factor
b. Plastic-zone correction	No

c. Values of Load and Crack Length Used

(1) Load at critical crack length

(2) Critical crack length = length at which crack began to extend with no increase in load

ALCOA

1. SPECIMEN					
a. Width	W (in.)	2	3	16	20
b. Length	L (in.)	12	14	44	60
c. Crack length	2a (in.)	0.66	1.0	1,2,3,4,6	1,3,7
d. Thickness	B (in.)	0.063	0.063, 0.125, 0.250	0.063, 0.125	1.0
2. NOTCH PREPARATION					
a. Size and shape					
b. How inserted		Milled	Milled	Milled and Jeweler's Sawcut	Brooch +0.001V
c. Fatigued		Yes	Yes	No	No
3. BUCKLING RESTRAINT					
a. Type		None			
b. When used		Never			
4. LOAD AND CRACK-LENGTH MEASUREMENT					
a. Load		Load Cell and Machine Recorder			
b. Crack length		Clip Gage and XY Plotter			
Gage length (in.)		2	2	10	17
5. DATA REDUCTION					
a. Equation		ASTM STP 410			
b. Plastic-zone correction		Yes	Yes	Yes, No	Yes
c. Values of load and crack length used					
(1) Load and crack length at instability					

BATTELLE

MIL-HDBK-5 TENTATIVE SUPPLEMENT September 1971

1. SPECIMEN

a. Width	W (in.)	$W \geqslant 9\ (K_{abb}/\sigma_{ys})^2$
b. Length	L (in.)	$L \geqslant 2W$
c. Crack length		$2a_c < W/3$
d. Thickness	B (in.)	No information

2. NOTCH PREPARATION

a. Size and shape	No information
b. How inserted	No information
c. Fatigued	Yes, $K_{fat} \geqslant K_{app}/2$

3. BUCKLING RESTRAINT

a. Type	No information
b. When used	No information

4. LOAD AND CRACK-LENGTH MEASUREMENT

a. Load	No information
b. Crack length	No information

5. DATA REDUCTION

a. Equation	$K_c = \sigma_G\sqrt{a_c\pi \sec(\pi a_c/W)}$
b. Plastic-zone correction	No information

c. Values of load and crack length used

(1) Maximum load initial crack length to give apparent K (K_{app})

(2) Limits: $\sigma_N < \sigma_{ys}$

$\sigma_G < 2/3\ \sigma_{ys}$

BOEING

1. TEST SPECIMEN

a. Width	W (in.)	As necessary, required, or available to satisfy data-use requirements
b. Length	L (in.)	L/W = 2.50 — 3.0 usually
c. Crack length	2a (in.)	$2a/W \leqslant 0.30$ for fracture test
d. Thickness	B (in.)	No information

2. NOTCH PREPARATION

a. Size and shape	Center hole diameter = .25 in., Width < 0.10 in.; Last 0.10 in. = 0.006 in. max. Length selected for either or both crack propagation and fracture tests
b. How inserted	Drill and saw cut
c. Fatigued	Yes; at about 1/3 of load at expected fracture level or 500 microinches/cycle

3. BUCKLING RESTRAINT

a. Type	Bars along crack on both sides of sheet
b. When used	For buckling — restrained data, otherwise satisfy design geometry and stress levels

4. LOAD AND CRACK MEASUREMENT

a. Load	Applied at about 1000 psi per second
b. Crack-length measurement	$2a_0$ through $2a_c$. Scale and telescope for growth. High-speed film for fracture.

5. DATA REDUCTION

a. Equation used	$K_c = \sigma \mathcal{G} \pi a \alpha$ (Irwin/Ishida/Secant)
b. Plastic-zone correction	$r = \left[2 \frac{1}{\pi} (K_c/\sigma_{ys})\right]^2$, as applicable

c. Values of load and crack length used to compute K_c specifically

(1) Load P and crack length 2a at instability maximum load and nonlinear range

(2) Load maximum and Initial crack length: P_m and $2a_0$ also used

FRANKFORD ARSENAL

"Relation of Crack Opening Stretch and Thickness Contraction to R-Curve for Evaluating Fracture Toughness"

C.C. Carman and G.R. Irwin Report R-2029, December 1971

1. SPECIMEN

a. Width	W (in.)	9
b. Length	L (in.)	No information
c. Crack length	(in.)	No information
d. Thickness	B (in.)	0.05, 0.125, 0.250

2. NOTCH PREPARATION

a. Size and shape	No information
b. How inserted	No information
c. Fatigued	Yes; at low stress

3. BUCKLING RESTRAINTS

a. Type	Plates covering both sides of sheet and bolted together; cut out window around initial crack and part of projected path
b. When used	Always

4. LOAD AND CRACK-LENGTH MEASUREMENT

a. Load	MTS closed-loop, servo-controlled machine Displacement control: 50 microinches per second
b. Crack length	Double cantilever beam gage calibrated for specimen

5. DATA REDUCTION

a. Equation	$K = YP/BW^{1/2}$, Isida
b. Plastic-zone correction	No; "effective" crack length measured
c. Values of load and crack length used	No information

MCDONNEL DOUGLAS

REFERENCE 14

1. SPECIMEN

a. Width		2 8 22 32 (most 22 in.)
b. Length	L (in.)	L = 3W
c. Crack Length	(in.)	Reported as 2a/W = 0.1, 0.2, 0.3
d. Thickness	B (in.)	0.05; 0.10; 0.2; 0.45; 0.6; 0.75 All machined from 0.75-in. stock All same heat; heat treated same time

2. NOTCH PREPARATION

a. Size and shape	No information
b. How inserted	"Starter" notches
c. Fatigued	Yes; unidirectional (R = 0.1) Gross stress at desired crack length: 10 ksi

3. BUCKLING RESTRAINTS

a. Type	No information
b. When used	On 0.05-in. specimens only

4. LOAD AND CRACK-LENGTH MEASUREMENT

a. Load	Applied 20 ksi/min
b. Crack-length measurement	Compliance and close range photographs (35-mm camera) at intervals coordinated with load by means of a Beckman recorder which also recorded the compliance gage output

5. DATA REDUCTION

a. Equation

$$K_c = \sigma\sqrt{W \tan(\pi a/W)}$$

$$K_c' = \sigma\left[1 - \left(\frac{\sin(\pi a/W)}{\sin\{(\pi/W)[a + (1/2\,\pi)]\}}\right)^2\right]^{-1/2}$$

$$K_c' = \sigma\sqrt{W \tan(\pi a/W)} + 1$$

b. Plastic-zone correction

c. Values of load and crack length used

Maximum load?

Both initial and final crack lengths

NASA — LANGLEY

1. SPECIMEN

a. Width	W (in.)	2	8	12
b. Length	L (in.)	12-5/8	24	35
c. Crack length	2a (in.)	0.5 — 1.6	0.25 — 5.0	0.25 — 6.1
d. Thickness	B (in.)	0.025 — 0.09	0.025 — 0.25	0.09 — 0.50

2. NOTCH PREPARATION

a. Size and shape

b. How inserted — Electric discharge

c. Fatigued — Yes

3. BUCKLING RESTRAINT

a. Type — Solid guide plates, front and back
Slit provided for crack-growth observation

b. When used — $B < 0.25$ in.

4. LOAD AND CRACK-LENGTH MEASUREMENT

a. Load — Recording oscillograph, calibrated load readout unit, maximum-load indicating needle on testing machine

b. Crack length — High-speed camera; visual

5. DATA REDUCTION

a. Equation used — $K_c = \sigma_G \sqrt{a_c \pi \sec (\pi a_c / W)}$

b. Plastic-zone correction — None

c. Values of load and crack length used

Load and crack length at instability if available

NRL

1. TEST SPECIMEN
   a. Width W (in.) 3 5 6 9 10 12 15 16 20
   b. Length L (in.)
   c. Crack length 2a (in.) Varied 2a/W: 0.083 → .50
   d. Thickness B (in.) Varied: 0.032 → 0.25

2. NOTCH PREPARATION
   a. Size and shape Width .0625 in. 60° L Tip
   b. How inserted Elox
   c. Fatigued Only a few

3. BUCKLING RESTRAINT
   a. Type
   b. When used All B < 0.090 in.

4. LOAD AND CRACK-LENGTH MEASUREMENT
   a. Load Microformer in load train to XY recorder
   b. Crack length Probe (described) in specimen slit to XY recorder

5. DATA REDUCTION
   a. Equation $K = \sigma\sqrt{a}\ 1.77\left[1-0.1\left(\frac{2a}{W}\right)+\left(\frac{2a}{W}\right)^2\right]$, ASTM STP 410
   b. Plastic-zone correction included by crack-length measurement
   c. Values of load and crack length used
      (1) Load and crack length at instability*
         *(a) Maximum load when separation occurs at maximum load
         (b) First values at maximum load when separation occurs after crack extension at constant load

NORTHRUP

NOR-69-169 May 1971

1. TEST SPECIMEN

a. Width	W (in.)	5.0
b. Length	L (in.)	18.5
c. Crack length	2a (in.)	.5; 1.5; 2.5; 3.5
d. Thickness	B (in.)	.032; .063

2. NOTCH PREPARATION

a. Size and shape

b. How prepared — Slotted with jeweler's saw from a 1/4-in. central hole to ≈ 80% of final length

c. Fatigued — Yes; MTS Universal Testing Machine
Sinusoidal, tension-tension ($R \approx O$) at a K value < 10 ksi$\sqrt{\text{in.}}$

3. BUCKLING RESTRAINT

Of 1/2 in. plexiglas covering the entire specimen; bolted with light wing-nut force

4. LOAD AND CRACK-LENGTH MEASUREMENT

a. Load — Machine to XY plotter

b. Crack length — Compliance gage XY plotter

Gage length — 0.280 in.

5. DATA REDUCTION

a. Equation

$$K = \sigma\sqrt{a}\ 1.77 + 0.227\left(\frac{2a}{W}\right) - 0.51\left(\frac{2a}{W}\right)^2 + 2.7\left(\frac{2a}{W}\right)^3$$

b. Plastic-zone correction — Included by crack-length measurement

c. Values of load and crack length used

(1) Load and crack length at instability

REYNOLDS

1. SPECIMEN

a. Width	W (in.)	15
b. Length	L (in.)	30 to Pin Load Line
c. Crack length	(in.)	4.0
d. Thickness	B (in.)	0.080 — 0.500

2. NOTCH PREPARATION

a. Size and shape	0.040-in. slot to 0.012-in. slit
b. How inserted	Slat: jigsaw blade through 1/4-in.-dia. hole at center of specimen Slit: at slot tip, jeweler's saw and razor blade
c. Fatigued	No

3. BUCKLING RESTRAINT

a. Type	Cutouts for gage in 4-in. aluminum channels bolted together and faced with Teflon
b. When used	Necessary for tough aluminum at least to 0.15 in. thick and probably to 0.350 in.

4. LOAD AND CRACK-LENGTH MEASUREMENT

a. Load	Moseley XY recorder
b. Crack length	Determined with compliance calibration

5. DATA REDUCTION

a. Equation	$K_c = \sigma\sqrt{\pi a \sec(\pi a/W)}$
b. Plastic-zone correction	No; included in compliance calibration

c. Values of load and crack length used to compute K_c:

1. K^1 Load at 5% secant offset and $2a_0$
2. K^2 Load maximum and $2a_c$ at load max.
3. K^3 Load final and $2a_c$ at final load
4. K^4 Load maximum and $2a_0$

Security Classification

DOCUMENT CONTROL DATA - R & D

(Security classification of title, body of abstract and indexing annotation must be entered when the overall report is classified)

1. ORIGINATING ACTIVITY *(Corporate author)* Naval Research Laboratory Washington, D.C. 20375	2a. REPORT SECURITY CLASSIFICATION Unclassified 2b. GROUP

3. REPORT TITLE

A REVIEW OF THE PLANE-STRESS FRACTURE MECHANICS PARAMETER K_c DETERMINED USING THE CENTER-CRACKED TENSION SPECIMEN

4. DESCRIPTIVE NOTES *(Type of report and inclusive dates)*

Special review report.

5. AUTHOR(S) *(First name, middle initial, last name)*

Anna M. Sullivan and Charles N. Freed

6. REPORT DATE December 29, 1972	7a. TOTAL NO. OF PAGES 51	7b. NO. OF REFS 39
8a. CONTRACT OR GRANT NO. NRL Problems M01-24 and M01-28 b. PROJECT NO. WR 022-01-01 c. d.	9a. ORIGINATOR'S REPORT NUMBER(S) NRL Report 7460 9b. OTHER REPORT NO(S) *(Any other numbers that may be assigned this report)*	

10. DISTRIBUTION STATEMENT

Approved for public release; distribution unlimited.

11. SUPPLEMENTARY NOTES	12. SPONSORING MILITARY ACTIVITY Department of the Navy Naval Air Systems Command Washington, D.C. 20360

13. ABSTRACT

This review discusses the current status of the center-cracked tension (CCT) specimen as a means of determining the plane-stress fracture-mechanics parameter K_c. The effect of specimen geometry (width and crack length) together with that of specimen thickness is illustrated by examples from NRL research.

The experimental parameters employed at NRL are detailed together with those in use at other laboratories for the purpose of assisting in the development of a standard procedure for such testing so that data can be reliably compared.

DD FORM 1 NOV 65 1473 (PAGE 1)

S/N 0101-807-6801

Security Classification

Security Classification

14. KEY WORDS	LINK A ROLE	LINK A WT	LINK B ROLE	LINK B WT	LINK C ROLE	LINK C WT
Fracture mechanics parameter K_c						
Center-cracked tension specimen						
Crack-opening-displacement (COD) calibration						
Geometric variables						
Plane stress						
Fracture resistance						

DD FORM 1 NOV 65 1473 (BACK)
(PAGE 2)

Security Classification